*Geophys. J. Int.* (2006) **167,** 380–396 doi: 10.1111/j.1365-246X.2006.03105.x

# Relative importance of the Hercynian and post-Jurassic tectonic phases in the Saharan platform: a palaeomagnetic study of Jurassic sills in the Reggane Basin (Algeria)

B. Smith,[1] M. E. M. Derder,[2] B. Henry,[3] B. Bayou,[2] A. K. Yelles,[2] H. Djellit,[2] M. Amenna,[2] M. Garces,[4] E. Beamud,[4] J. P. Callot,[5] R. Eschard,[5] A. Chambers,[6] T. Aifa,[7] R. Ait Ouali[2,8] and H. Gandriche[9]

[1]*Laboratoire de Tectonophysique (CNRS UMR* 5568*), case* 049, *Université de Montpellier II,* 34095 *Montpellier cedex* 5, *France. E-mail: smith@dstu.univ-montp2.fr*
[2]*CRAAG., B.P.* 63, *Bouzaréah* 1640, *Alger, Algeria*
[3]*Paléomagnétisme, IPGP and CNRS,* 4 *avenue de Neptune,* 94107 *Saint-Maur cedex, France*
[4]*Group of Geodynamics and Basin Analysis, University of Barcelona, Facultat de Geologia, Campus de Pedralbes,* 08028-*Barcelona, Spain*
[5]*Institut Français du Pétrole, Geology-Geochemistry direction,* 1-4 *av. de Bois Préau,* 92852 *Rueil Malmaison cedex, France*
[6]*Repsol YPF Exploracion SA, Paseo de la Castellana* 280, 28046 *Madrid, Spain*
[7]*Géosciences, (CNRS UMR* 6118*), Université de Rennes* 1, *Campus de Beaulieu,* 35042 *Rennes cedex, France*
[8]*Université des Sciences et Techniques Houari Boumedienne, BP* 9, *Dar El Beida, Alger, Algeria*
[9]*SONATRACH, Exploration, Avenue du* 1[er] *novembre, Immeuble IAP, Boumerdes, Algeria*

Accepted 2006 June 9. Received 2006 June 8; in original form 2005 July 20



## SUMMARY

In the intracontinental domain of the northwestern Saharan platform, the deformation of the Palaeozoic sedimentary cover is mainly attributed to a far-field effect of the Hercynian orogeny having occurred at the African–Laurusian plate boundary in the Late Carboniferous to Early Permian times. However, geological observations from different parts of Africa and Arabia provide evidence that several minor but widespread tectonic events occurred later, particularly during the Cretaceous. Contrary to elsewhere in the northwestern part of Africa, in the Reggane Basin, outcropping doleritic sills of Early Jurassic age are intruded in folded Palaeozoic sediments of Devonian to Carboniferous ages deposited before the Hercynian orogeny. In this favourable situation, a palaeomagnetic study of the Liassic dolerite is able to provide information on the tectonic history of the surrounding area independently from geological observations.

The present study aims to quantify the relative proportion of tilting related to, respectively, the Hercynian and a post-intrusion phase, using a fold test based on the small circle analysis. This method proved to be very efficient to unravel these tectonic events. It shows that, in the studied area, the folds were initiated during the Hercynian phase, but mainly amplified during the post-intrusion phase which turned out to be the dominant one. In the Reggane Basin, the age of this second event is not geologically well constrained between probably Late Jurassic and Early Cretaceous. It could be the far-field effect of either the Cimmerian phase (∼140 Ma) or more likely the Austrian tectonic phase (Late Barremian, ∼125 Ma). The Late Barremian tectonic episode corresponds to a major event: the break-up of Western Gondwana, which led to the separation of Africa from South America and to the incipient fragmentation of the African plate into three major blocks. The conclusion drawn from the palaeomagnetic study in the Reggane Basin is consistent with the geological observations and representative of the intraplate Cretaceous deformations recorded in many other places in Africa. It emphasizes once again that stresses can be transferred far from the plate boundaries, into the continental plate interiors.

**Key words:** doleritic sill, Hercynian, Jurassic, palaeomagnetism, Saharan platform, tectonic phase.

## INTRODUCTION

In the western part of the Saharan platform in NW Africa, folding and faulting of the Palaeozoic sedimentary cover is usually considered to result mainly from the Hercynian tectonics (Beuf *et al.* 1971; Fabre 1976; Donzeau *et al.* 1981; Conrad & Lemosquet 1984). However, there has been recently growing evidence that several tectonic episodes occurred later in the Mesozoic Era, mainly during the Cretaceous (Conrad 1981; Guiraud *et al.* 1987; Guiraud & Maurin 1992; Boote *et al.* 1998; Guiraud *et al.* 2005). Deciphering between Hercynian and Cretaceous tectonic effect is often impossible, when deposits younger than the Late Palaeozoic are missing or have been eroded, like in a large part of the Ahnet and Mouydir Basins (Fig. 1a). The eastern border of the Reggane Basin is an interesting area because Liassic intrusive dolerites together with Jurassic and Cretaceous sediments have been preserved, and outcrop in some places. The age of the Early Liassic intrusions of doleritic basalts is well constrained, but the overlying Jurassic and Cretaceous sediments are imprecisely dated. Also, the outcrops of Jurassic rocks are of poor quality, which prevents from recovering reliable geological information.

This study aims to determine the relative proportion of tilting acquired during the tectonic events, which have occurred, respectively, before and after the dolerite emplacement, using a palaeomagnetic approach. The method consists in studying, in several sites of both limbs of a fold, the palaeomagnetic direction of a doleritic sill of Early Liassic age intruded in folded Devonian to Carboniferous layers. Assuming that the magnetization of the dolerite is primary, the small circle analysis (Surmont *et al.* 1990; Shipunov 1997) allows to determine at each site the dip of the surrounding layers (Hercynian dip) at the time of the dolerite emplacement. Subsequently, the dips generated by the post–intrusion event can be deduced.

The fold test commonly used in Palaeomagnetism (e.g. McFadden 1990; Watson & Enkin 1993; Tauxe & Watson 1994; Shipunov 1997) is a powerful test that allows to date the magnetization acquisition time relative to tectonic tilting. Applied to a sedimentary layer, this technique assumes that the primary magnetization is blocked during the horizontal deposition of the strata or that the horizontal plane during deposition is known. However, when a sill is intruded parallel to the bedding of a sedimentary formation, if the layers are presently folded at the outcrop, it is instructive to know whether the surrounding sediments were horizontal, already fully tilted, or only partly tilted compared as today, at the time of the magmatic intrusion. If the sill is sampled in several sites of various dips, in both limbs of a fold, the direction of its primary magnetization can lead to the reconstruction of the fold geometry when this magnetization was blocked (Delaunay *et al.* 2002; Henry *et al.* 2004a), that is, when the dolerite was intruded. Thus, in case of polyphase tectonics, it can allow to better understand the kinematics of each one of the regional tectonic events (McClelland-Brown 1983; Surmont *et al.* 1990; Stamatakos & Hirt 1994; Jordanova *et al.* 2001).

This paper then focuses on two subjects of broad interest. The first one concerns the structural implications (including the domain of hydrocarbons investigation) of the relative importance of the Hercynian and Mesozoic tectonics for the whole northern part of Africa. The second one is related to the method itself, which is here applied for the first time in such a geological context.

## GEOLOGICAL SETTING

Convergence between Laurussia and Gondwana in the Carboniferous-Early Permian times led to the Hercynian and Appalachian–Mauritanides orogeny which is responsible for the formation of the Maghrebian and Mauritanides fold belts in the West African margin. Far from the belt, in the intracontinental

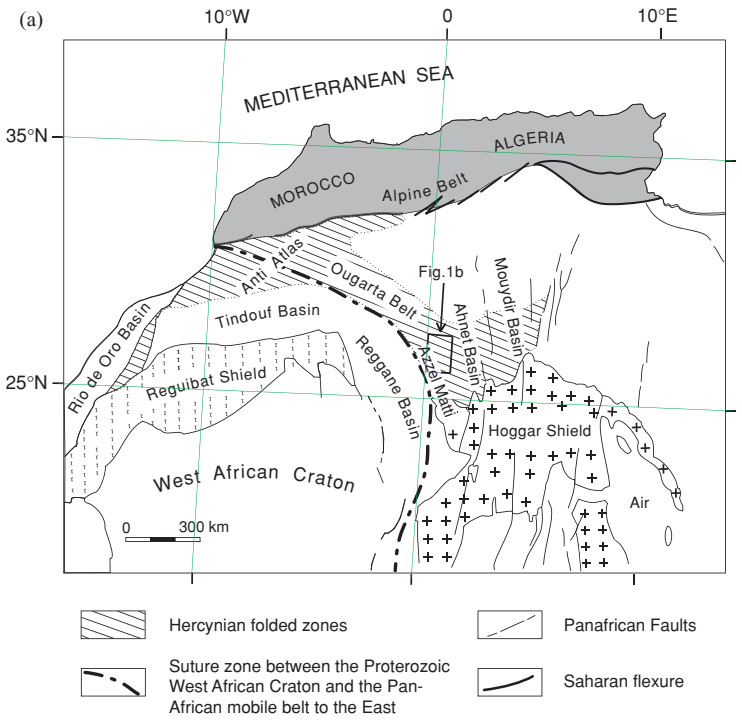


**Figure 1.** Presentation of the studied area. (a) Simplified structural map of NW Africa, modified from Conrad (1981). (b) Geological map of the studied area redrawn from Bensalah *et al.* (1972). Dashed lines represent hidden faults. (c) Geological cross section in the studied area.

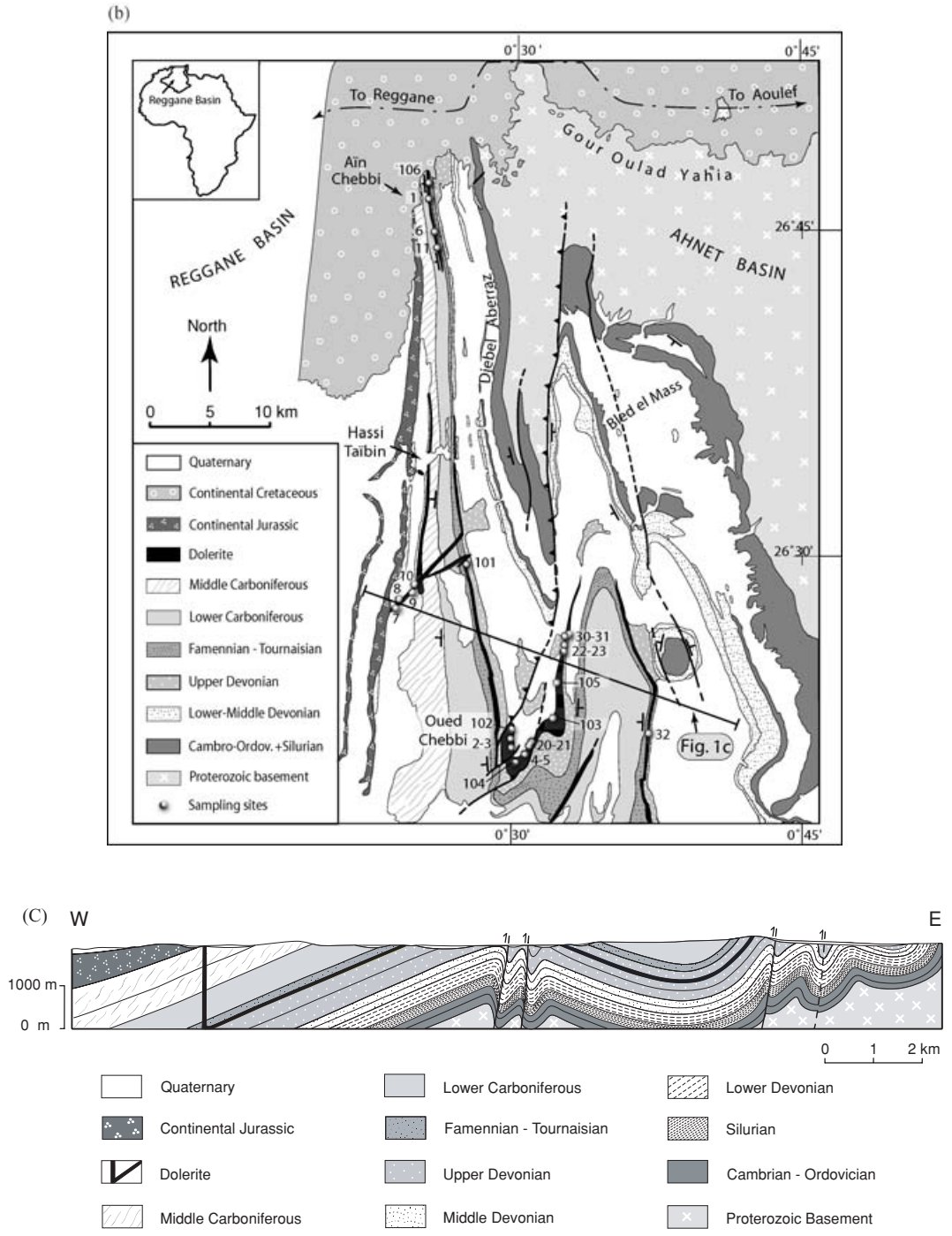


**Figure 1.** (*Continued*.)

domain of the West African craton and the central to eastern Saharan platform, the Hercynian deformation is generally weak and mainly expressed as gentle monoclinal structures, saddles, arches and intervening sag basins. However the Ougarta–Ahnet region of Algeria (Figs 1a and b) is largely folded (Donzeau *et al.* 1981), probably due to the reactivation of the underlying suture zone (Caby *et al.* 1981) between the West African craton (2000 Ma) and the Hoggar shield stabilized after the Pan-African orogeny (600 Ma) (Fig. 1a). According to Conrad (1981), this boundary would have remained unstable during the whole Phanerozoic times. In the Reggane, Ahnet and Mouydir Basins, the Hercynian deformation is expressed by folded areas separated by subvertical N–S to NW–SE strike slip and reverse faults cross-cutting the basement (Fig. 1c). The compressional and transpressional structures observed in these basins allowed to determine a NE–SW shortening direction (Haddoum *et al.* 2001; Zazoun 2001), interpreted by these authors as far field stress effects of the Hercynian orogeny. In this region, the folding is probably Early Permian (Conrad & Lemosquet 1984; Fabre 1988; Haddoum *et al.* 2001). The deformation of the Palaeozoic cover is mainly the superficial expression of horizontal

and vertical displacements along ancient Pan-African fracture zones in the basement (Beuf *et al.* 1971; Fabre 1976; Donzeau *et al.* 1981). This is particularly true for the submeridian Bled el Mass-Azzel Matti fault zone (Figs 1a, b) which corresponds to rejuvenated Pan-African sutures (Black *et al.* 1979; Caby 1987).

In the Early Mesozoic, a period of major lithospheric extension led to the initial break-up of the Pangea supercontinent. During the Late Triassic–Early Jurassic, rifting developed the passive margins of the future Central Atlantic Ocean (Manspeizer 1988) and the eastern and northern margins of Africa–Arabia with the opening of the Western Neotethys (Guiraud *et al.* 1987). Related to this rifting phase and prior to the beginning of seafloor spreading in the Early Middle Jurassic (Vogt & Einwich 1979), an extensive episode of basaltic magmatism produced sill and dike intrusions and volcanism. It affected a wide domain (Central Atlantic Magmatic Province) in West Africa (Black & Girod 1970; Cogney *et al.* 1971; Bardon *et al.* 1973; Logan & Duddy 1998; Wilson & Guiraud 1998) as well as in South and North America (Sutter 1988) and Iberia (Cebria *et al.* 2003). In Africa, this magmatism led to intrusion of dolerite, which extends from Morocco and Algeria to the Ivory Coast and is mainly localized to the west and north of the West African craton. These dolerites form a very homogeneous compositional group and display identical mineralogical, textural and chemical features over distances exceeding 1500 km (Black & Girod 1970). According to Bertrand & Westphal (1977), these dolerites are quartzitic tholeiites and very similar to those outcropping in the Appalachians, particularly in the New Jersey. In Africa, K–Ar dating determined on dikes and sills from Morocco (Hailwood & Mitchell 1971; Westphal *et al.* 1979) and in Liberia (Dalrymple *et al.* 1975) are all well constrained within the interval 180–200 Ma. An extensive review of the radiometric dating determined on the Early Jurassic volcanics from NW Africa has been published by Sebaï *et al.* (1991) and Verati *et al.* (2005) who reinvestigated the timing of this magmatic event using the $^{40}Ar/^{39}Ar$ radiochronological method. They obtained very narrow plateau ages peaking around 198.1 Ma on dykes and sills from the Taoudeni area in Mali and on lava flows in Morocco. The Foum Zguid dike of the Moroccan Anti-Atlas and the Ksi-Ksou dike of Algeria are dated, respectively, at 196.9 $\pm$ 1.8 Ma and 198.0 $\pm$ 1.8 Ma (Sebaï *et al.* 1991). The outstandingly well grouped ages of these dolerites together with their homogeneous geochemical composition (Sebaï *et al.* 1991; Verati *et al.* 2005) demonstrate that they have been emplaced in a very short time as it was suggested by White *et al.* (1987). The thermal history of the Reggane and Ahnet Basins, based on apatite and zircon fission track analyses combined with organic reflectance measurements throughout the Phanerozoic rocks, clearly shows a sharp thermal peak between 195 and 205 Ma (Logan & Duddy 1998).

Along the eastern border of the Reggane Basin in the Bled-el-Mass–Azzel Matti region of Algeria (Figs 1a and b), these dolerites outcrop either as several sills interlayered within the folded Palaeozoic sedimentary cover which unconformably overlies the upper Proterozoic Pan-African basement, or as dikes cross-cutting this series or feeding the sills. Thickness of the sills is mostly of the order of 15 to 20 m, but may be locally as thin as 5 m.

In this area and in the surrounding regions of Ahnet and Mouydir (Fig. 1a), Conrad (1972, 1981) and Lefranc & Guiraud (1990) described another tectonic event having occurred after the dolerite injection. The deformation associated with the post-dolerite phase is represented by frequent uplift and block tilting, minor folding and drag folds along the N–S basement faults, and underlined by hiatuses and unconformities (Guiraud *et al.* 2005). In the studied area (Figs 1b and c), the Late Namurian layers and the dolerites are unconformably overlaid by a moderately dipping and discordant series of a continental Formation of probably Late Jurassic age. The base of this Formation is constituted by a fluviatile conglomerate which includes pebbles from the underlying Palaeozoic formations, fragments of doleritic basalts and elements from Proterozoic rocks (Conrad 1972). On the field (Fig. 1b), the dip of this conglomerate and its relationship with the underlying Carboniferous series is difficult to measure, due to the poor quality of the rare preserved outcrops. It decreases from about 30°–50° in the northern Aïn Chebbi area to 18°–24° south from Hassi Taïbin, where the Jurassic Formation overlays a doleritic dike (Fig. 1b). North of the Reggane Basin, this series is sealed by horizontal continental deposits (Continental Intercalaire) whose age is Early Cretaceous in this area (De Lapparent 1960; Conrad (1981), Lefranc & Guiraud (1990)). The age of the tectonic phase postdating the dolerite intrusion should thus be constrained between the Early Jurassic and the Early Cretaceous. This tectonic event can thus be an expression of the instability of the African plate at the beginning of Early Cretaceous (Cimmerian phase, Guiraud & Bosworth 1999), as mentioned in Conrad (1981) and Lefranc & Guiraud (1990). It can also be a far-field effect of the Late Early Cretaceous (Austrian rifting phase), which affected a large part of the African plate (Fairhead 1988; Guiraud & Maurin 1991, 1992; Boote *et al.* 1998).

Preliminary studies on the Early Liassic dolerites of the Reggane Basin were carried out by Conrad & Westphal (1973) on only two samples (Aïn Chebbi area) and by Bardon *et al.* (1973) in three sites (less than 10 samples). In both studies, the dip of the sills was not given and no tilt correction was applied to the data. Therefore these data cannot be taken into account in the present study.

## SAMPLING

The sampling was carried out with two objectives in mind: sample the same chronological unit in order to avoid secular variation effects and allow the fold test to be performed in the most favourable conditions, that is, with different bedding azimuths and dips in the two limbs of the fold. Cooling models for a basaltic flow or a magmatic intrusion (Carslaw & Jaeger 1959; Turcotte & Schubert 1982; Smith *et al.* 1991) shows that, for a sill of 20 m thick, the cooling time is of the order of one year maximum, which is equivalent to a spot reading of the Earth's magnetic field.

Two injection phases can be inferred from field observations, although they probably closely follow each other: 8 km south from Hassi Taïbin (Fig. 1b), the NE–SW trending dike crosscuts, and thus postdates, a N–S trending sill injected into the Namurian gypsum layers. Eastwards, this dike, which is injected along a fault plane, branches out into two dikes, also following fault planes. Each one of these dikes feed a N–S sill interlayered into Upper Famennian clayey formations (Conrad 1972). The north propagating sill is interrupted around the latitude of Hassi Taïbin, and it is likely the same sill which reappears in the north, around Aïn Chebbi, interlayered in the Visean–Tournaisian clayey units. In this area, one can observe this sill passing from one stratigraphic level to another one.

Sampling sites are not as widely distributed along the intrusion bodies as could have been expected because the dolerites do not outcrop properly everywhere and because they are often weathered. Furthermore, part of the outcrops lie in areas of unsafe access.

The 24 sampling sites (251 samples) reported on Fig. 1(b) correspond only to fresh outcrops. They have been collected during

independent field trips (sites with number between 1 and 23 by Algiers–Montpellier–Saint-Maur group, sites 30 to 32 by Rennes team and sites 101–106 by Barcelona–Rueil-Malmaison team). They are mainly spread along the southern sill in the Djebel Aberraz anticline and in the adjoining Bled-el-Mass syncline (16 sites) and in the feeding dyke (4 sites). Four more sites have been sampled in the area of Aïn Chebbi in order to add steep dipping sites to the collection of moderately dipping sites. All the samples were oriented by magnetic and solar compass. The number of samples per site is 4 to 6 cores (Rennes sampling), between 10 and 16 cores (Algiers–Montpellier-Saint-Maur sampling) and 4 to 5 hand samples, giving a total of 11 to 13 cores (Barcelona–Rueil-Malmaison sampling). One to three specimens of standard size (cylinders of 11 $cm^3$) were cut from each sample, generally allowing palaeomagnetic and rock magnetic analyses to be performed.

## EXPERIMENTAL PROCEDURE

In order to characterize the magnetic minerals five polished thin sections were examined under reflected light, then submitted to electron microprobe analyses. Thermomagnetic analyses were performed on 15 samples, including the ones analysed by scanning electron microprobe, with a Bartington magnetic susceptibility meter operating in a field of 80 A $m^{-1}$ and under vacuum, in order to determine the Curie temperatures of the magnetic minerals. Finally, five stepwise thermal demagnetizations of a three axes isothermal remanent magnetization (IRM) as described in Lowrie (1990) were performed, after application of fields of 0.9 T, 0.14 T and 0.06 T, respectively, along Z, Y and X.

Prior to any demagnetization analysis, the specimens were stored in a zero magnetic field for one month, in order to reduce a possible viscous remanent magnetization (VRM). The remanent magnetization was measured using a CTF cryogenic magnetometer settled in a shielded amagnetic room whose maximum residual field is lower than several hundreds of nT. All the samples were thoroughly thermally or AF demagnetized. AF demagnetizations were carried out on a laboratory-built demagnetizer described in Le Goff (1985). Thermal treatments were performed in a non-inductive furnace in which the residual field is less than 10 nT. In order to correctly isolate and identify the magnetization components, numerous steps were performed, with increments ranging from 50°C in the lowest temperatures to 10°C in the highest one, up to 590°–610°C for the thermal treatment, and from 5 nT to 20 mT up to 100 to 160 mT for the AF demagnetization. The magnetic susceptibility (K) was measured at room temperature after each heating step in order to monitor possible mineralogical changes having occurred upon heating. The demagnetization process is presented on orthogonal vector plots (Wilson & Everitt 1963; Zijderveld 1967). When clearly identified, the direction of the characteristic remanent magnetization component (ChRM) was calculated by principal component analysis (Kirschvink 1980), otherwise remagnetization circles (Halls 1976, 1978) were used when the unblocking temperature (or field) spectra of two adjoining magnetization components partly or totally overlap. At the site level, the mean characteristic directions were calculated using Fisher's statistics (Fisher 1953) and combined analysis of ChRM and remagnetization circles (Bailey & Halls 1984; McFadden & McElhinny 1988). Small circle analysis (Surmont *et al.* 1990; Shipunov 1997; Henry *et al.* 2004a) was finally used to determine at the same time the average primary magnetization direction of the dolerites and the amplitude of each one of the tectonic phases having affected each sampling site.

## MAGNETIC MINERAL AND ROCK MAGNETIC INVESTIGATIONS

### Microscope observations and electron microprobe analyses

The examination of polished thin sections confirms that the rocks are holocrystalline dolerites with an ophitic texture, while chemical analyses carried out by Khouas (1998) classifies them in the quartz tholeiitic basalt with a composition at the boundary between the mid-ocean ridge basalts (MORB) and the island arc tholeiites (IAT). This is consistent with the analyses of Moroccan dolerites carried by Bertrand & Westphal (1977). Observation in reflected light reveals a between-site variation in the opaque mineralogy, but also sometimes from one sample to the other within a single site. Indeed, the oxide mineral assemblage varies from point to point in a single magmatic unit, depending on the position of the sample relative to the chilled margin, the cooling rate and the oxygen fugacity (Haggerty 1976).

However, several common features can be summarized as follows. The samples contain numerous titanomagnetites from two generations: The small ones are spread in the matrix or underline silicate contours. They seem to be homogeneous and often automorph and angular but they are usually too small ($<1$ to few $\mu$m) to be unambiguously identified. The large ones (50–500 $\mu$m in size) develop subautomorphic contours with two distinct features: if the sample come from the outer quenched part of the sill (Fig. 2a), the titanomagnetites, although much larger, resemble those described in submarine basalts with skeletal and cruciform to euhedral shapes. They are apparently homogeneous and exsolution free. However, small shrinkage cracks develop from the grain margins, indicative of an incipient low temperature oxidation. If the sample come from the more slowly cooled inner part of the sill or dyke (Fig. 2b) the titanomagnetites can reach 0.5 mm in size and exhibit a dense network of trellis-like intergrowths of ilmenite lamellae into the residual Ti-poor titanomagnetite. The oxidation degree does not generally exceed the C3 stage defined by Buddington & Lindsley (1964) and Haggerty (1976). Fresh and homogeneous euhedral to subhedral crystals (10–100 $\mu$m) of ilmenite laths sometimes ending in a graphic texture (sandwich types and composite types of Buddington & Lindsley 1964; Haggerty 1976; Lindsley 1991) are frequent and indicate both a primary crystallization and an oxidation-exsolution process in the same rock sample. Sulfide granulations (5–20 $\mu$m) are also common, often developed inside or against the titanomagnetite crystals.

Electron microprobe analyses were carried out on three coarse grained polished section to determine the chemical composition of the magnetic oxides. 10 to 15 grains of exsolved titanomagnetites were analysed in each sample with a number of analyses varying from 3 to 16 per individual grain, depending on the crystal size. Several independent grains of ilmenite were also analysed, confirming their presumed composition. Unfortunately, because the oxy-exsolution lamellae are very fine, that is under the separating power of the electron beam, these analyses represent only a mixture of several mineralogical phases. Few analyses were also carried out in a fine-grained dolerite where the titanomagnetites have squeletal shapes and shrinkage cracks. The average composition corresponds to a titanomagnetite close to $x = 0.6$ with very little substitutions (metal content in weight per cent: Fe = 54–55 per cent; Ti = 12 per cent; Al = 1 per cent; Mg = 0.1 per cent; Mn = 0.3 per cent). The sum of the oxide percentage is 96–97 per cent (expected to be $100 \pm 1.5$ per cent for a stoichoimetric titanomagnetite) indicating

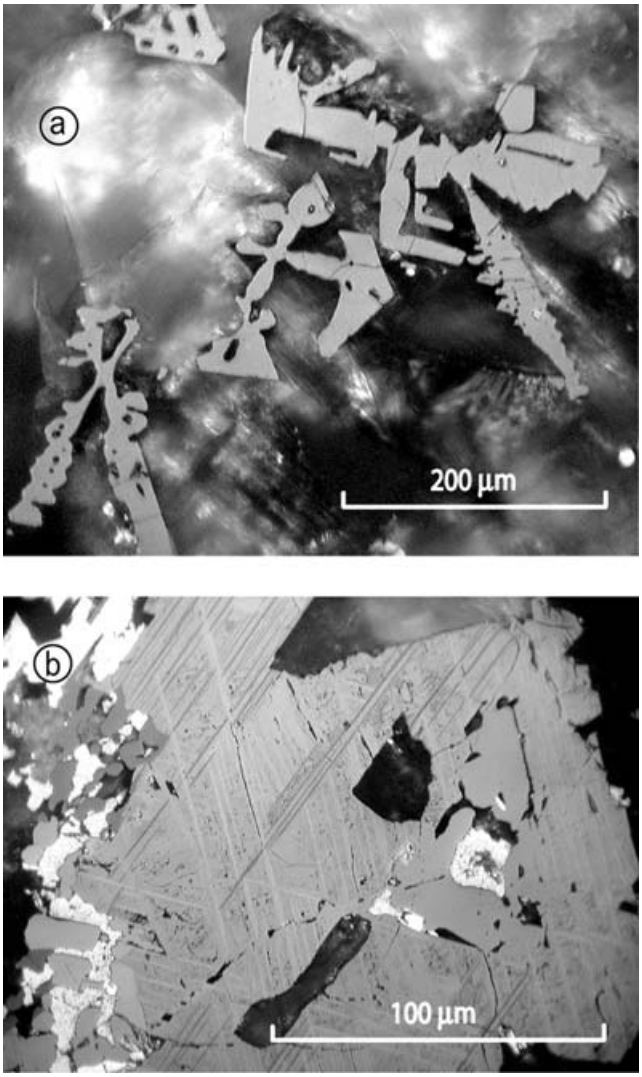


**Figure 2.** Microscope examination of titanomagnetites in reflected light. (a) Squeletal shape titanomagnetites displaying few low temperature shrinkage cracks. (b) High-temperature oxidation of titanomagnetite showing exsolutions of ilmenite and Ti-poor titanomagnetite in the (111) cristallographic planes. Sulfides are also present, inside and along the titanomagnetite border (white areas).

that the titano-magnetite has been low temperature oxidized into a titanomaghemite.

### Rock magnetic characterization of the magnetic carriers

In order to fully understand the characteristics of the magnetic grains responsible for the magnetization, it is necessary to examine together the information provided by polished thin sections, thermomagnetic curves, temperature changes of the room temperature magnetic susceptibility after thermal treatment, natural remanent magnetization (NRM) thermal decay curves, acquisition of the saturation IRM and thermal demagnetization of the three axes IRM experiments (Lowrie 1990).

All the doleritic samples saturate in relatively low fields (between 0.3 Tand 0.9 T). Upon thermal demagnetization, the soft IRM component (acquisition field: 60 mT) is the largest one, the IRM acquired in 140 mT the intermediate one, and the IRM blocked in the strongest field (0.9T) the weakest one. This is to be expected for samples containing magnetic minerals of the titanomagnetites series. However, the samples can be classified in different groups according to their behaviour.

In the coarsest grained samples (sites 2, 5, 10, 20), where the high-temperature oxy-exsolutions are well developed, thermomagnetic curves are almost reversible with either a single or two Curie temperatures.

If there is a single (or major) Curie temperature (Tc), the thermomagnetic curves are almost reversible. Tc varies between of 540°C and 575°C upon heating (Fig. 3a). The NRM thermal demagnetization curve shows a dominant unblocking temperature spectrum below about 550°C, and sometimes also a minor one around 300°–400°C (Fig. 4a), while the magnetic susceptibility measured at room temperature after each heating step displays only minor changes during heating. AF demagnetization reveals that coercivities extend up to values higher than 100 mT, and thermal demagnetization of the 3 axes IRM shows that the soft, intermediate and hard fractions have maximum unblocking temperatures of 540°–550°C (Fig. 5a). All these observations are consistent with high-temperature exsolutions of titanomagnetite and ilmenite (Fig. 2b), and support the presence of essentially a fine grained Ti-poor titanomagnetite close to the magnetite composition ($x \sim 0$).

In other sites or samples, the thermomagnetic curves can be slightly to clearly irreversible, with two Curie temperatures (sites 1, 2, 5, 9, 10, 11, 20, 23, 31 and 32): the first one is between 250°C and 350°C and disappears upon cooling, the second one around 550°–570°C (Fig. 3b). The NRM thermal decay evidences two unblocking temperature spectra (Fig. 4b) consistent with the thermomagnetic recordings. The room temperature magnetic susceptibility evolves generally little during the whole thermal treatment, but the changes occur as early as about 200°C (Fig. 4b) consistent with the thermomagnetic recording. Thermal demagnetization of the three axes IRM (Fig. 5b) indicates that the maximum unblocking temperatures are close to 300°C and 550°C for, respectively, the first and the second population of magnetic minerals. This is again consistent with the Tc curves and the NRM thermal decay curves. These observations together with the shrinkage cracks observed in some of the titanomagnetites of this kind of sample suggest that a titanomaghemite was initially present, together with a Ti poor titanomagnetite intergrown with ilmenite lamellae. These two populations of magnetic grains are likely to cover the single domain (SD) to pseudo-single domain (PSD) range, according to their coercivity spectra.

In the finest grained dolerites (sites 6, 11), the strong irreversibility of the thermomagnetic curves above 200°C (Fig. 3c) is corroborated by the large changes of the room temperature susceptibility above 200°C (Fig. 4c): between 200°C and 400°C new ferrimagnetic minerals are formed, whereas from 400°C to 550°C, ferrimagnetic minerals are destroyed or inverted into more weakly or non magnetic phase. Tc recording and NRM thermal decay curve suggest again the presence of two populations of magnetic minerals: the first one is probably a titanomaghemite which inverts upon heating. This is substantiated by the observation of shrinkage cracks in the squeletal shaped titanomagnetites in the fine-grained dolerites (Fig. 2a). The second one may be a Ti poor magnetite according to the Curie temperatures of 550°C and the maximum unblocking temperature of 560°C. The lowest coercivities are found in these samples, as indicated by the thermal demagnetization of the three IRM (Fig. 5c) and by the AF demagnetizations in which the main part of the NRM is unblocked by magnetic fields lower than 50 mT. This suggests that the microscopic size of the magnetic grains is as

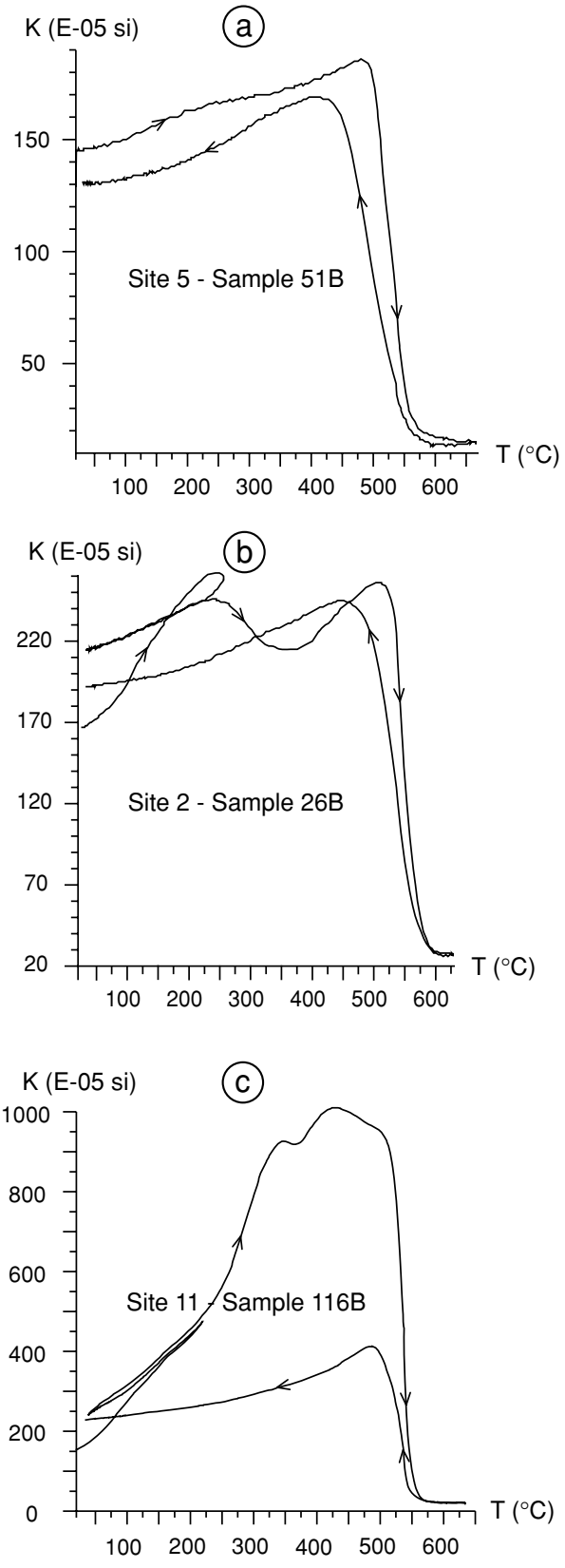


**Figure 3.** Thermomagnetic curves under vacuum of typical samples. (a) Almost reversible curve of Ti-poor magnetite. (b) Irreversible curve showing Titanomaghemite and Ti-poor magnetite. (c) Strongly irreversible thermomagnetic curve evidencing large mineralogical changes. K is the volume susceptibility.

a whole larger in these samples than in the coarse-grained dolerites where oxy-exsolutions are present.

## PALAEOMAGNETIC STUDY: IDENTIFICATION OF THE MAGNETIZATION COMPONENTS

### General remarks

According to the rock magnetic investigations, the dolerites can be expected to exhibit at least two distinct magnetization components: one carried by a titanomaghemite, the other by a Ti-poor magnetite. Thermal treatment was more efficient to isolate these components, because their unblocking temperature spectra are offset from each other while the unblocking fields are mostly overlapping, although they are slightly lower for the titanomaghemite component. However, secondary IRM due to lightning are widespread in the dolerites from the Reggane Basin, and thus AF demagnetization had often to be used to selectively remove this remagnetization. In few sites, the overprinting was total so that no other magnetization component could be retrieved (sites 7, 8, 21). These sites were thus discarded. In other sites, the remagnetization was only partial and/or did not concern all the samples, so that the ChRM component could be reached through AF treatment (sites 3, 5, 6, 9, 11, 22, 23, 30 and 31). For the remaining samples, thermal treatment was applied.

The quality of the palaeomagnetic recording is clearly related to the amount of Ti-poor titanomagnetite relative to the quantity of titanomaghemite, as seen through the unblocking temperatures spectra: when the sample contains a large amount of titanomaghemite and correlatively a small quantity of magnetite, the magnetization is found to be the more noisy, and prone to VRM or recent CRM acquisition, whereas large changes of the susceptibility occur upon heating. Conversely, the best palaeomagnetic recordings are those of samples containing the largest amount of Ti-poor magnetite.

### Identification of the magnetization components

Apart from lightning IRMs, three magnetization components can be generally identified, all of normal polarity. Occasionally a fourth small "crypto" component of reversed polarity can be detected, squeezed between the two highest unblocking temperature components.

*Component A* is widespread in the samples (or sites) which have not been struck by lightning. It is usually small relative to the NRM, except at sites 22, 23, 30 and 31 were it represents from $\frac{1}{4}$ to $\frac{1}{2}$ of the original NRM intensity. Its unblocking temperatures ($T_{\mathrm{ubs}}$) usually span the interval 100 to 250°–280°C, but can sometimes extend much higher temperatures (sites 22, 23, 30 and 31). The *in situ* mean directions are well gathered ($D = 359.7°, I = 43.2°$, $\alpha_{95} = 1.5°, k = 1039$, for $n = 10$ sites, Fig. 6a) and close to the present dipole field normal direction ($I = \pm 44.9°$ at 26.5°N latitude) while they scatter upon dip correction (Fig. 6b). It is either a VRM or a CRM of recent origin (Henry *et al.* 2004b).

*Component B* could rarely be isolated by AF (unblocking fields, $H_{\mathrm{ubs}}$, essentially in the range 25 mT to 50 mT), but most efficiently by thermal treatment, in the intermediate unblocking temperature range ($280°\mathrm{C} \leq T_{\mathrm{ubs}} \leq 380°$–$400°\mathrm{C}$). It has been determined in 11 sites (Table 1), is always associated to component C, but isolated in a smaller number of samples because the unblocking temperature/field spectra of components B and C partly overlap (Fig. 4c) and the two directions are very close to each other (Figs 4a and b). On

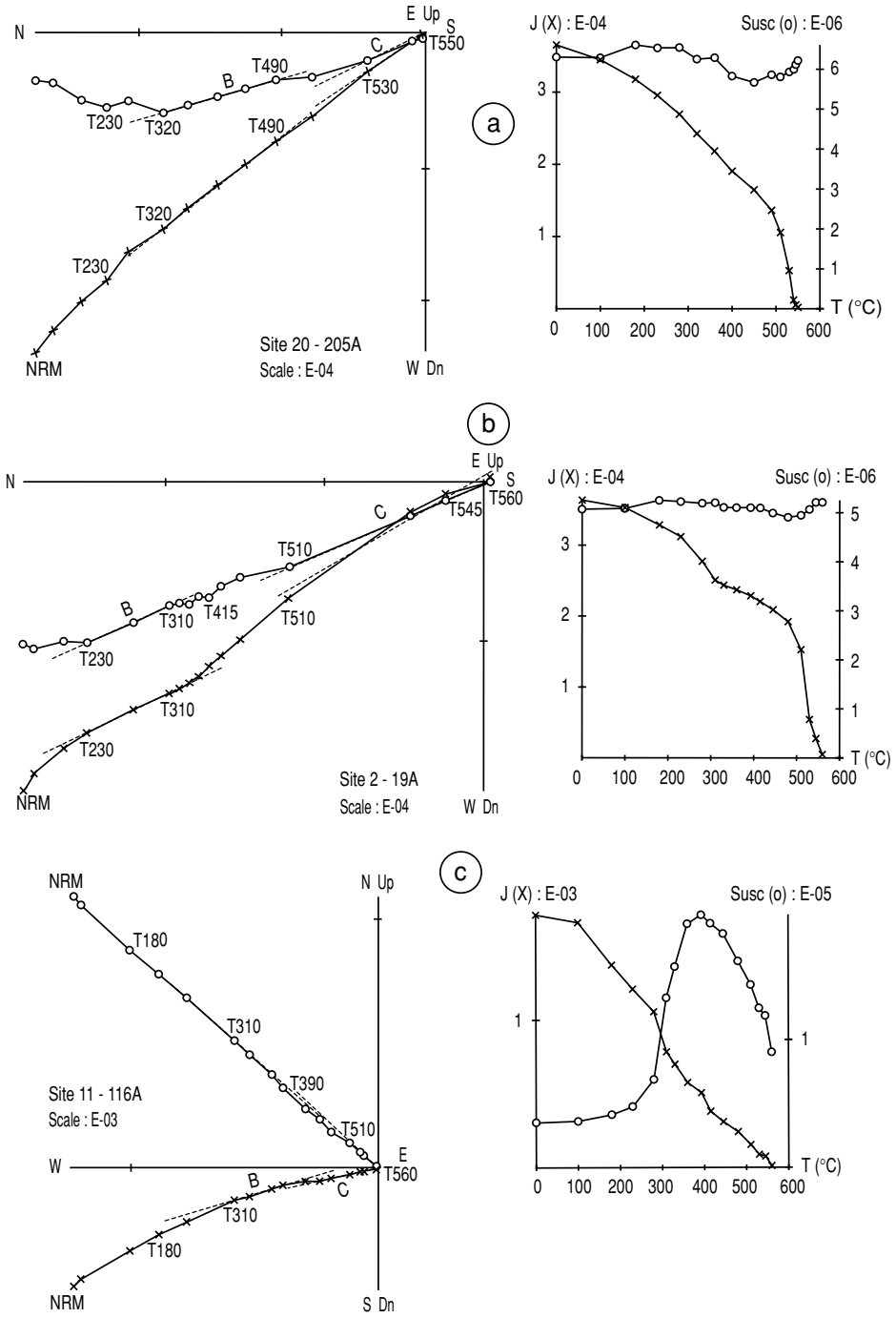


**Figure 4.** Orthogonal vector plots in stratigraphic coordinates together with NRM intensity decrease and susceptibility changes as a function of temperature, for three samples corresponding, respectively, to the three types of thermomagnetic curves shown in Fig. 3. Open circles and crosses represent, respectively, horizontal and vertical planes, then susceptibility and NRM. The susceptibility is here the mass susceptibility, expressed as $m^3\ kg^{-1}$.

the grounds of its unblocking temperatures, microscope observations and rock magnetic analyses, it is likely that the magnetization component B is carried by titanomaghemite, probably in the PSD to MD range. Because the occurrence of the recent A component is linked with that of the B component, it is possible that A and the B magnetization components are both carried by the titanomaghemite. This titanomaghemite may correspond to the skeletal shape titanomagnetite seen in the finest grained dolerites, and maybe also to the second generation of the small oxides which are often numerous in the matrix but too small ($\leq 1\ \mu$m) to be identified. As maghemitization generally occurs after the original crystallization of the rock, component B is expected to be a secondary magnetization component.

The existence of a '*reversed crypto component*' can be postulated in six sites (sites 1, 22, 23, 30 and 31). In most samples, its $T_{ub}$ spectrum overlap with those of the adjacent components and its direction could be determined in only 8 samples from 3 sites. This component is well constrained in the range of 400°–450°C to 490°C.

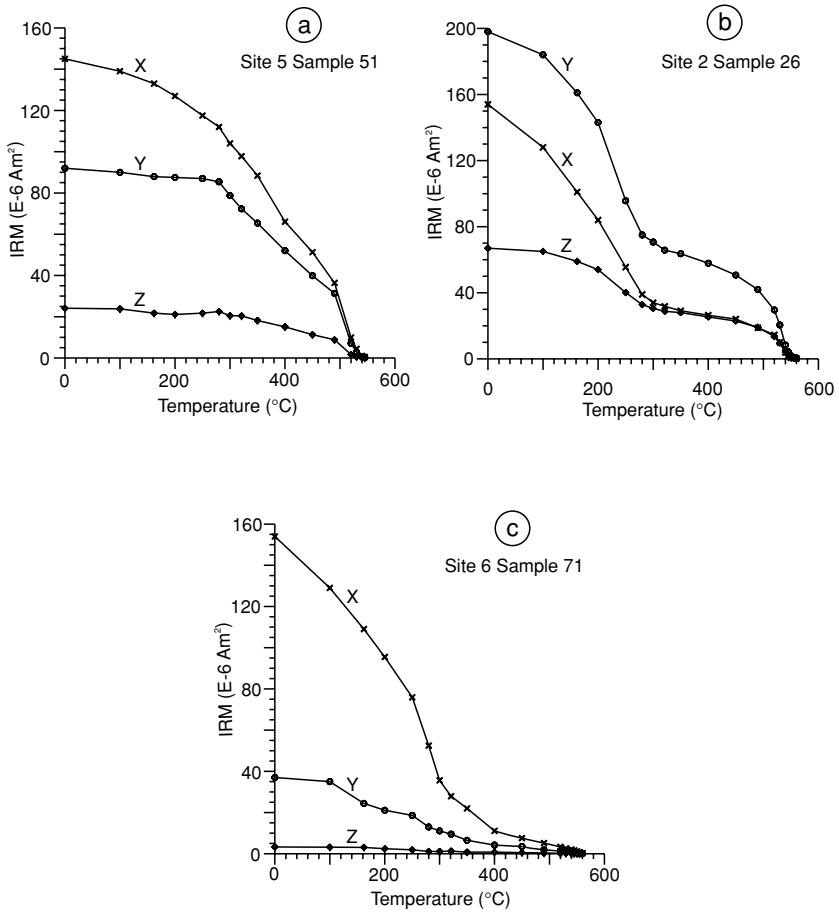


**Figure 5.** Thermal demagnetization of three axes IRM, according to Lowrie (1990). Fields of 0.9 T, 0.14 T and 0.06 T have been applied, respectively, along Z, Y and X. a, b and c represent, respectively, the three types of samples displayed in Figs 3 and 4.

It is clearly of reversed polarity and seems to be roughly opposite to the B or C component with an average direction of $D = 174.8^\circ$, $I = -32.1^\circ, \alpha_{95} = 8.6^\circ, k = 43$ and $D = 178.4^\circ, I = -33.6^\circ, \alpha_{95} = 10.6^\circ, k = 28$, respectively, before and after tilt correction. However, this direction is imprecise because it is determined through only two or three demagnetization steps. Therefore, this component cannot be considered any further in the scope of this paper. It is worth noting that if this component is opposite to the C one, it constitutes an interesting phenomenon in a volcanic unit which is expected to cool more rapidly than the time required for a magnetic reversal to occur. It suggests a possible negative interaction between two adjacent oxy-exsolutions phases leading to a self-reversal magnetization of one of the ferrimagnetic phase.

*Component C* spans both the highest unblocking temperatures (480°–500°C $\leq T_{ubs} \leq$ 550°–575 °C) and the highest unblocking field intervals (30–40 mT $\leq H_{ubs} \leq$ 120 mT up to possibly 170 mT). It is ubiquitous, as long as lightning has not struck the sites and consequently is found in the majority of samples from 20 sites (Table 2), but its intensity relative to the original NRM can be highly variable. In some samples, only great circles have been determined (Table 2). Component C is probably carried by the fine elongated exsolutions of Ti-poor titanomagnetite, likely in the SD to PSD range, as deduced from the previous observations and rock magnetic experiments. It is thus contemporaneous of the dolerite injection and consequently it is probably of primary origin.

### The particular case of the magnetization directions at sites 22, 23, 30 and 31

In these neighbour sites (Fig. 1), only few samples provide apparently acceptable ChRMs directions while most of the other samples had to be discarded for the following reasons. The orthogonal plots are generally complex, suggesting sometimes the presence of more than three components, most often overlapping. It is in these sites that the reversed-crypto component is found in several samples. Two main behaviours are observed.

In the majority of samples the recent A remagnetization has generally the largest intensity relative to the B and C components which are much reduced, and often noisy (Fig. 7a). In these samples, the two orthogonal plots display sigmoidal shapes which are characteristics of a total overlap of one component over the next one. Here, the A component totally envelops the others. It can be isolated not only in the lowest but also in the highest unblocking temperature range were it has completely remagnetized the C component. An intermediate direction, with a declination shifted to the east, is obtained in the intermediate $T_{ubs}$, as a result of overlapping of A with B (Fig. 7a). These samples have been discarded. Consequently no reliable ChRM remains in site 30, out of the four samples collected.

In the remaining few samples, the intensity of the C component is large enough compared to the one of component A but the unblocking range of component A can again extend up to the highest temperature so that the A and C $T_{ubs}$ can also overlap. These samples display a more westerly declination and have been retained in

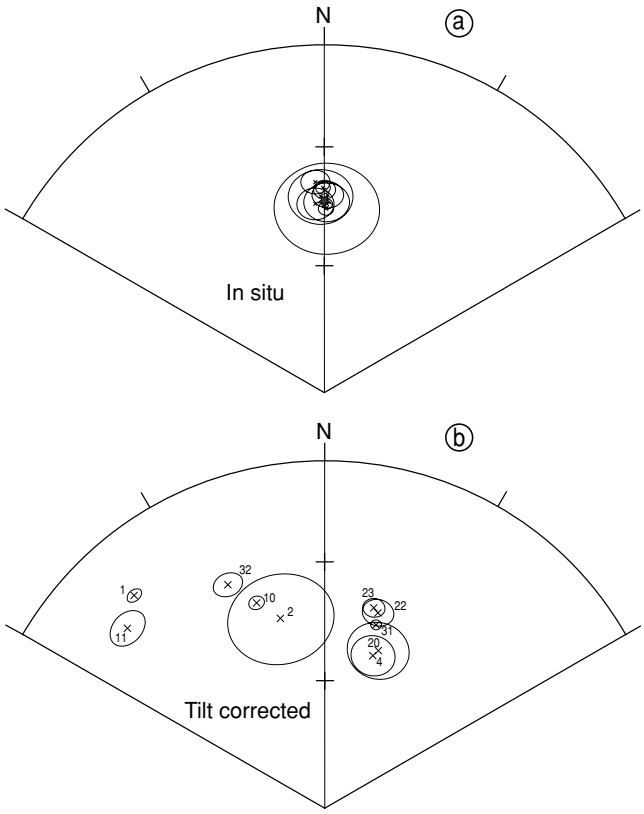


**Figure 6.** Site mean directions of component A and associated $\alpha_{95}$. (a) *In situ* coordinates. The star represents the present dipole field. (b) After tilt correction, with the site numbers indicated.

**Table 1.** Site mean directions of Component B (titanomaghemite) in the Reggane dolerites. *n* is the number of ChRMs.

| | | *In situ* coordinates | | | | After full tilt correction | | | |
|---|---|---|---|---|---|---|---|---|---|
| Site | *n* | $D_g$ | $I_g$ | $\alpha_{95}$ | *k* | $D_s$ | $I_s$ | $\alpha_{95}$ | *k* |
| 1 | 7 | 352.1 | 40.3 | 3.9 | 246 | 316.7 | 13.8 | 3.9 | 246 |
| 11 | 6 | 337.6 | 32.4 | 6.8 | 97 | 316.9 | 5.3 | 6.8 | 97 |
| 10 | 6 | 346.3 | 44.2 | 1.8 | 1464 | 331.6 | 32.0 | 1.8 | 1464 |
| 2 | 6 | 341.2 | 25.6 | 4.1 | 266 | 335.9 | 19.6 | 4.1 | 266 |
| 4 | 6 | 331.4 | 20.0 | 3.1 | 481 | 335.6 | 35.1 | 3.1 | 481 |
| 5 | 5 | 324.6 | 18.6 | 4.8 | 259 | 327.3 | 34.5 | 4.8 | 259 |
| 20 | 5 | 329.5 | 21.9 | 3.9 | 387 | 335.7 | 38.9 | 3.9 | 387 |
| 22 | 3 | 349.5 | 41.5 | 9.5 | 169 | 4.1 | 43.6 | 9.5 | 170 |
| 23 | 4 | 349.6 | 33.2 | 7.7 | 142 | 0.5 | 35.8 | 7.7 | 142 |
| 31 | 3 | 353.6 | 37.5 | 2.4 | 2630 | 5.5 | 39.5 | 2.4 | 2630 |
| 32 | 5 | 347.3 | 31.3 | 2.6 | 885 | 333.7 | 19.7 | 2.6 | 885 |
| **All sites** | **11** | **341.4** | **31.9** | **7.1** | **43** | **337.1** | **30.0** | **11.1** | **18** |

the present study, although the C component may still be somewhat biased by the A remagnetization. One sample, with apparently no $T_{\text{ubs}}$ overlap, is shown in Fig. 7(b). It is noteworthy that the western declination of this sample is in better agreement with those of all the other sites, than the other samples from sites 22, 23, 30 and 31.

## ChRM and fold tests

If, for a given site, we compare the directions of components B (Table 1 and Fig. 8) and C (Table 2 and Fig. 9), respectively, before and after tectonic correction, the individual site mean directions are never significantly different at the 95 per cent level, except in 3 sites where the confidence angles for components B and C are tangent to each other. If, for each one of the sites, the directions of components B and C are not statistically different, it means that these components have almost the same age. This suggests that maghemitization occurred soon after the magma cooling, that is shortly after the dolerite injection. However, the declinations and inclinations of the B component are consistently higher than that of the C component, thus closer to the present field direction in geographic coordinate. This suggests a possible overlap of the unblocking fields or temperatures of the A and B components. It is indeed observed in most orthogonal projection plots, particularly in sites 22, 23, 30 and 31.

As the purpose of this work is to find the palaeo-attitude of the intruded layers at the time of the dolerite emplacement, we will afterwards focus on the primary C magnetization component alone. Fig. 9 shows that the *in situ* site mean directions of components C are rather scattered but the dispersion increases when the directions are tilt corrected. In order to check this visual estimation, we performed the fold test of McFadden & Jones (1981) on component C, testing whether the overall mean direction for the two families of opposite dips can be statistically distinguished before and after tilt correction. Therefore, we gathered in two groups the west and east dipping sites. The results indicate that the null hypothesis of a common true mean direction may be rejected both before and after tilt correction: the value calculated using McFadden & Jones (1981) equation is always higher than the critical value for the 95 per cent degree of significance ($0.408 > 0.283$ and $0.955 > 0.283$, respectively, in geographic and in stratigraphic coordinates). The fold test is thus negative, before dip correction as well as after total tilt correction. This demonstrates that the dolerites were not injected when the Palaeozoic sequence was already tilted as it is today (*in situ* directions) nor were they emplaced when the Palaeozoic layers were still horizontal (tilt corrected directions), but with some intermediate dips. This first conclusion supports the geological observations that at least one tectonic phase affected the Reggane Basin after the emplacement of the dolerites.

When the fold test is negative before and after tilt correction, a synfolding magnetization is commonly assumed. The tests as proposed for example by Johnson & Van der Voo (1989), McFadden (1990), Bazhenov & Shipunov (1991), Watson & Enkin (1993) and Tauxe & Watson (1994) imply proportional untilting on the two limbs. Implementation of this method leads to the best clustering of the directions for 35 per cent untilting of the 20 sites, with $D = 331.5^\circ, I = 30.3^\circ, \alpha_{95} = 1.5^\circ, k = 45$. However, as emphasized by Bazhenov & Shipunov (1991) there is no geological evidence that the two limbs of a fold are always tilted symmetrically about its hinge line during the fold amplification. This is obviously not always true, as is shown for example in Jordanova *et al.* (2001), Henry *et al.* (2001, 2004a), or in asymmetrical folds (Delaunay *et al.* 2002). Here, the geological map shows that the folded structure is indeed not perfectly cylindrical. An examination of the site mean directions before and after tilt correction (Fig. 9) reveals two points: first the groups of sites with comparable dips and belonging to a same area behave roughly similarly upon untilting. Second, these groups of sites require differential unfolding of the different part of the structure in order to get the best clustering of their site mean ChRMs. In this situation, proportional untilting of the ChRMs of all the sites does not make sense, and the general pattern of the bedding attitudes at the time of the dolerite intrusion can only be achieved through the small circle analysis as described by McClelland-Brown (1983), Surmont *et al.* (1990) and Shipunov (1997). During

**Table 2.** Site mean directions of Component C (magnetite) in the Reggane dolerites. $N$ = total number of samples: $n$ = number of ChRMs; $n'$ = number of great circles.

| | | *In situ* coordinates | | | | After full tilt correction | | | |
|---|---|---|---|---|---|---|---|---|---|
| Site | $N = (n + n')$ | $D_g$ | $I_g$ | $\alpha_{95}$ | $k$ | $D_s$ | $I_s$ | $\alpha_{95}$ | $k$ |
| 1 | 9 (9+0) | 348.1 | 40.2 | 4.8 | 116 | 315.6 | 11.0 | 4.8 | 116 |
| 106 | 11 | 337.5 | 33.3 | 2.8 | 270 | 315.3 | 6.7 | 2.8 | 270 |
| 6 | 11 (9+2) | 349.5 | 34.3 | 6.7 | 49 | 318.5 | 13.0 | 6.6 | 49 |
| 11 | 8 (8+0) | 335.8 | 35.5 | 4.6 | 145 | 313.5 | 5.7 | 4.6 | 145 |
| 9 | 8 (5+3) | 339.8 | 45.3 | 3.4 | 277 | 326.1 | 31.2 | 3.4 | 278 |
| 10 | 15 (15+0) | 341.2 | 41.6 | 2.7 | 207 | 328.8 | 28.1 | 2.7 | 207 |
| 101 | 10 | 323.2 | 27.2 | 6.7 | 54 | 314.3 | 21.6 | 6.7 | 54 |
| 102 | 12 | 328.5 | 25.7 | 3.7 | 137 | 326.4 | 40.4 | 3.7 | 137 |
| 2 | 13 (13+0) | 337.5 | 32.8 | 3.7 | 127 | 330.6 | 25.9 | 3.7 | 127 |
| 3 | 7 (2+5) | 327.0 | 38.3 | 8.4 | 64 | 319.9 | 29.2 | 8.4 | 64 |
| 104 | 9 | 330.8 | 27.7 | 5.3 | 96 | 325.5 | 13.3 | 5.3 | 96 |
| 4 | 10 (10+0) | 328.4 | 15.5 | 3.8 | 162 | 331.4 | 31.1 | 3.8 | 162 |
| 5 | 10 (10+0) | 321.9 | 14.5 | 2.8 | 290 | 324.0 | 30.7 | 2.8 | 290 |
| 20 | 9 (9+0) | 326.6 | 17.1 | 4.7 | 123 | 331.3 | 34.7 | 4.7 | 123 |
| 103 | 13 | 324.4 | 19.9 | 5.0 | 70 | 322.1 | 28.0 | 5.3 | 62 |
| 105 | 8 | 327.8 | 31.7 | 5.3 | 110 | 336.8 | 42.6 | 5.3 | 110 |
| 22 | 3 (3+0) | 341.9 | 35.6 | 11.5 | 116 | 353.9 | 40.2 | 11.5 | 116 |
| 23 | 8 (8+0) | 348.2 | 30.8 | 5.4 | 105 | 358.2 | 33.9 | 5.4 | 105 |
| 31 | 3 (3+0) | 347.9 | 34.4 | 2.7 | 2100 | 358.7 | 38.2 | 2.7 | 2100 |
| 32 | 6 (6+0) | 341.0 | 32.9 | 3.7 | 334 | 327.9 | 18.5 | 3.7 | 334 |
| **All sites** | **20** | **334.9** | **31.0** | **4.7** | **48** | **328.0** | **26.8** | **6.7** | **24** |

untilting of the limbs of a fold, the magnetization directions evolve along small circles centred on the fold axis. The intersection of the small circles of different sites with different bedding azimuths represents theoretically the single possible common magnetization direction acquired during the whole deformation. The best intersection of small circles may thus correspond on each circle to a different partial tilt correction. The dip value used for this partial unfolding (called here 'Hercynian dip') is supposed to represent the dip of the site at the magnetization acquisition time (Jordanova *et al.* 2001; Henry *et al.* 2004a). If two flanks of a cylindrical fold are sampled and if the same magnetization is recorded in both limbs, the small circles should be tightly parallel to each other instead of intersecting, and the mean synfolding magnetization can be undetermined along the small circle if the fold has been rotated around its axis. We can thus reconstruct the relative geometry of the limbs of the fold at the magnetization blocking time, but not their absolute attitude relative to the horizontal plane.

## DISCUSSION AND STRUCTURAL IMPLICATIONS

The dolerite intruded into its surrounding host Palaeozoic sediments is folded in an asymmetrical structure (Fig. 1b) forming an anticline to the west, followed by a syncline to the east. The weakly tilted periclinal termination is slightly refolded, as a result of displacement along secondary faults. Most of our samples come from the anticline, which is characterized by a long western flank and a short eastern one, but also by high dips in the north, regularly decreasing toward the south down to the periclinal termination. The dips measured at all the sampling sites allow to reconstruct the anticline structure and to determine that the main fold axis is approximately inclined by 5° to the south, along a N179° strike. The question thus arises as to whether the fold axis has been tilted after the dolerite intrusion or if it was already tilted when the dolerite was emplaced. In the first case, the ChRM directions should be corrected for the fold axis inclination, while in the second they should not. This answer can be provided by the consistency between the geological arguments and the small circle analysis performed in the different bedding attitudes.

Due to the poor outcropping conditions, the geological information is limited. We only know that the post-dolerite conglomerate is markedly tilted in the northern area of Aïn Chebbi, and that its dip decreases regularly to almost horizontal toward the southernmost outcrops. Therefore, the post dolerite tectonic phase ($\varphi 2$) is important in the northern part of the Reggane Basin. This conglomerate constitutes the first deposits of probably Late Jurassic age (Conrad 1981) following the dolerite intrusion. In the Hassi Taïbin area where it is best outcropping, Moussine-Pouchkine (personal communication) observed graded bedding with an inverse stratigraphy: the largest blocks at the base come from the closest upper Palaeozoic formations and also include pebbles of dolerite, while the finest detrital elements of the top come from the more remote Proterozoic basement. This stratigraphic sorting suggests that the conglomerate has formed in response to an important uplift to the NE as proposed by Conrad (1981), or to the N in the Late Triassic to Early Jurassic, according to Logan & Duddy (1998), while the surrounding area was simultaneously eroded.

The effect of the Hercynian phase ($\varphi 1$) must have been also more intense in the north than in the south in order to explain the present dips usually exceeding 60° around Aïn Chebbi. This is consistent with the presence of an uplifted zone which already existed during the Carboniferous, south of the Ougarta aulacogen in the Bled-el-Mass and western Ahnet Basin, which separated the two subsiding Basins of Reggane and Ahnet, according to Conrad & Lemosquet (1984). This first tectonic phase would have initiated a dissymmetrical fold with higher dips in the north, decreasing toward the south, with an axis inclined by 5° toward the South.

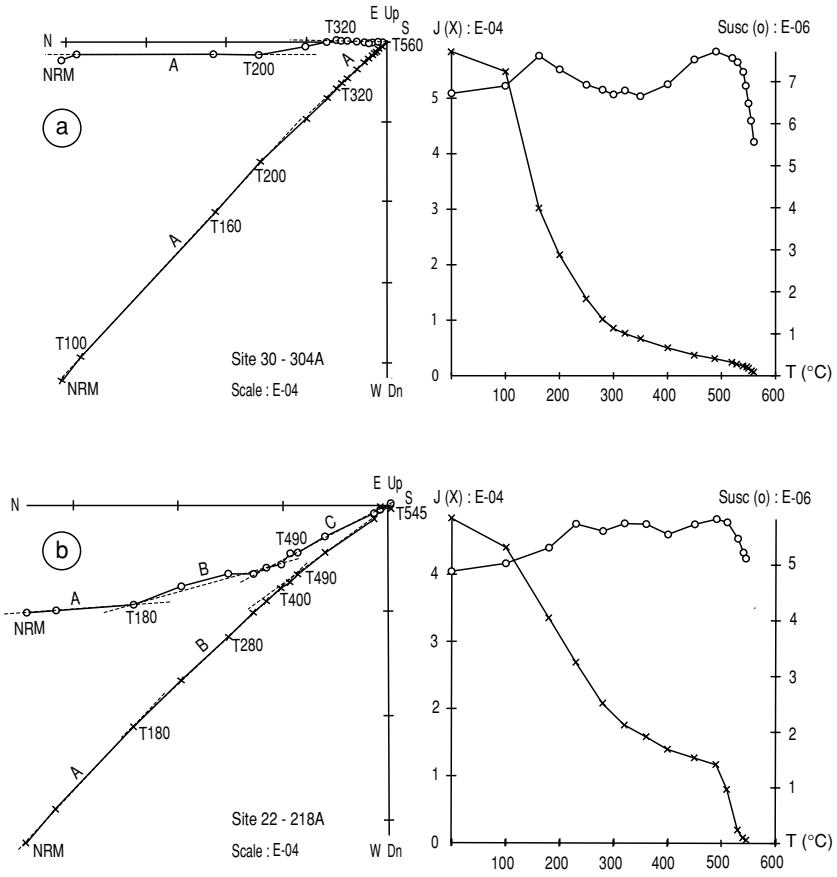


**Figure 7.** Orthogonal vector plots in geographic coordinates together with NRM and susceptibility changes upon heating in the two types of samples observed in sites 22, 23, 30 and 31. Same legend as in Fig. 4. (a) The unblocking temperature spectrum of component A is totally enveloping the other components (bad sample). (b) The unblocking spectra of components A, B and C can be separated (good sample). Note the difference in Declination in the high-temperature components of the two samples, and the difference in the NRM decay curve: in the bad sample compared to the good one, the amount of magnetite is smaller and correlatively the proportion of titanomaghemite higher.

The intersection of small circles, respectively, with and without correction of the fold axis inclination confirms that the fold axis dip should not be corrected, implying that the fold was originally tilted since the Hercynian phase: correcting for the fold axis plunge implies a weak post-dolerite tilt in the Aïn Chebbi area, which is at variance with the present dip of the Late Jurassic conglomerate. The same qualitative results are obtained if the tilt correction is limited to 0–100 per cent unfolding. In the present context of a polyphase tectonics, an unlimited tilt correction (beyond 0 and 100 per cent) must be allowed (Fig. 10).

### Restoring the layers in their relative attitudes at the time of the dolerite injection

Two sites deserve a special mention because they are south dipping with a strike almost perpendicular to the general fold axis strike and consequently, play an important role in the location of the intersection of the small circles: Site 102 is just south from the NE–SW trending Hercynian fault against which the dolerite abuts (Fig. 11a). According to the small circle analysis, this site would have been entirely tilted by the Hercynian phase (Fig. 11b). Site 103 is situated in the gentle subsidiary anticline inside the eastern limb of the main anticline. It would have been tilted partly before but mainly after the dolerite emplacement (Fig. 11b). Site 103 behaves similarly as the neighbour sites 4, 5, 20, except for the dip azimuth. The directions of these two sites (particularly site 102) evolve in the area of intersection of most the other small circles, so that they do not affect the expected direction. Therefore, these sites will be kept in the next calculations.

### Assumption 1: All the sites are taken into account ($N = 20$ sites)

The small circle analysis was first performed on the C component of all the sites ($N = 20$). The results are illustrated in Figs 10(a) and 11(b) and quantified in Table 3. The intersection direction ($D = 328.0^\circ, I = 26.6^\circ, \alpha_{95} = 1.6^\circ, k = 382$) is only 4.8° apart from the direction calculated for 35 per cent of proportional untilting of the same sites. However, the overall feature characterizing Fig. 10(a) is the broad area covered by the circles and consequently the large uncertainty around the intersection direction assumed to represent the Early Jurassic magnetic field in this area. It must be reminded that the small circle method is an optimization approach, in which the Fisher's parameters are calculated for idealized directions, so that they do not represent the true dispersion. They are therefore underestimated. The small circle analysis applied to all the sites leads to the following structural implications.

*Effects of the Hercynian phase* ($\varphi 1$): When the dolerites were emplaced after $\varphi 1$, the anticline structure of the Djebel Aberraz (Fig. 1b) and the adjacent Bled-el-Mass syncline were already

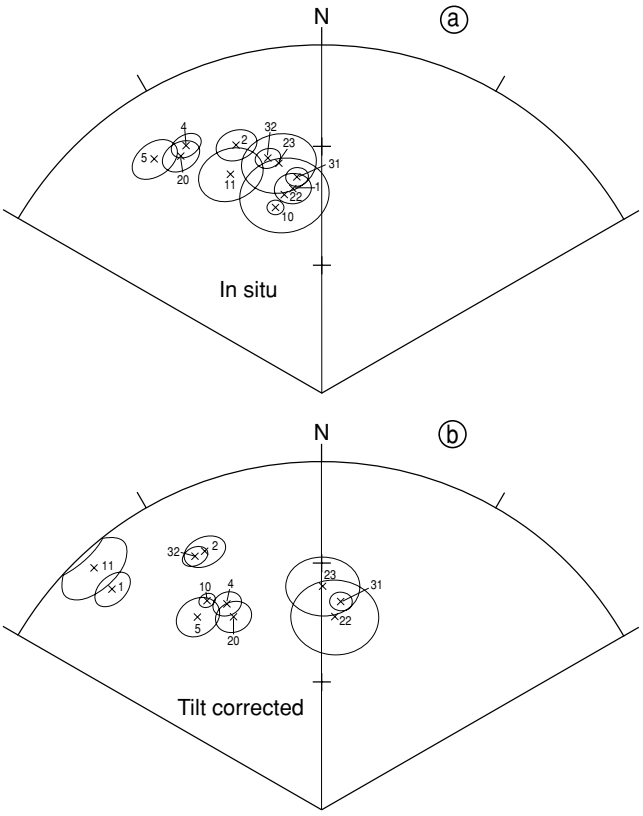


**Figure 8.** Site mean directions of component B (titanomaghemite). (a) *In situ* coordinates. (b) After tilt correction. Same legend as in Fig. 6.

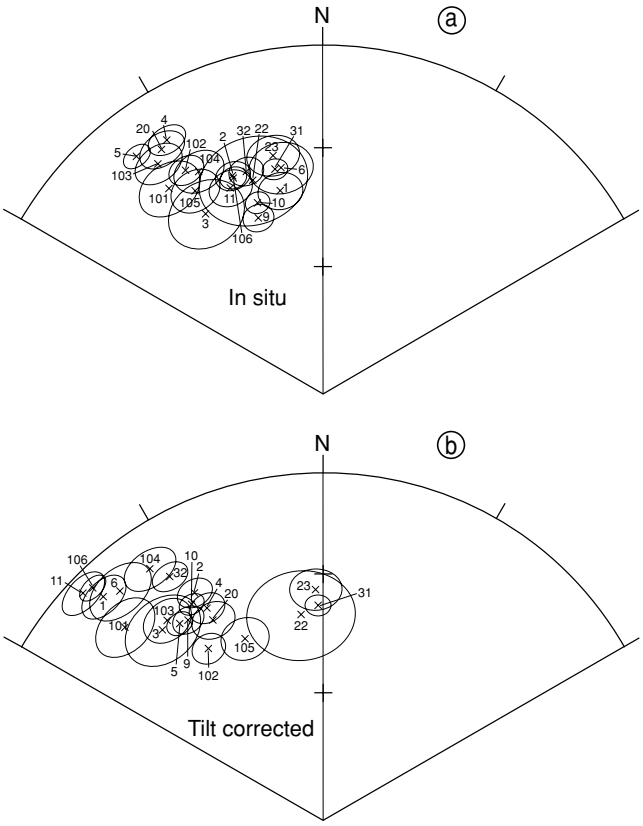


**Figure 9.** Site mean directions of component C (magnetite). (a) *In situ* coordinates. (b) After tilt correction. Same legend as in Fig. 6.

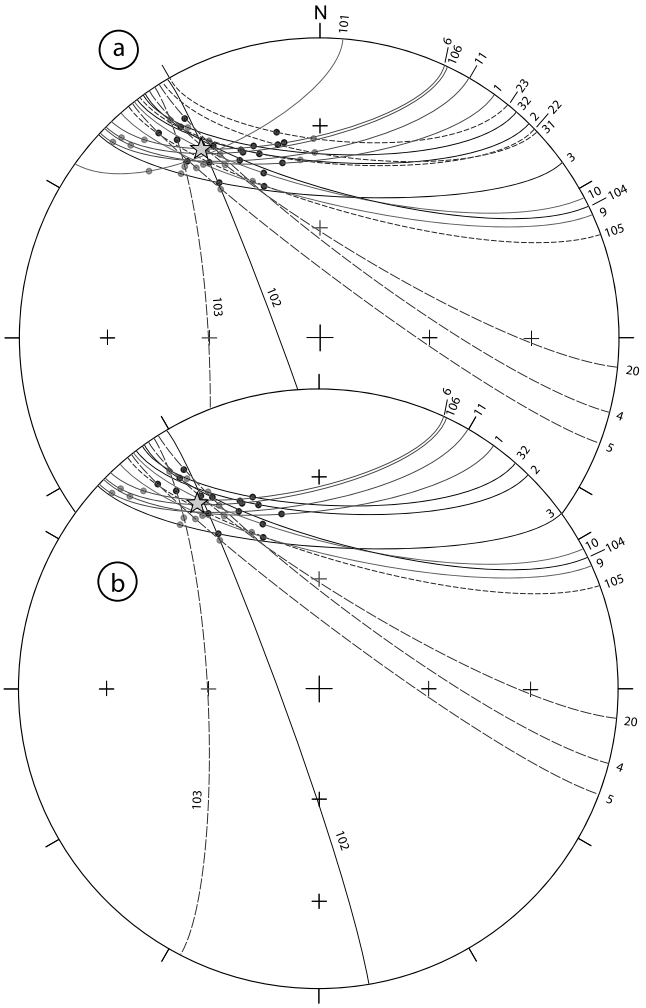


**Figure 10.** Small circle analysis. (a) All the sites ($n = 20$). (b) Without sites 22, 23, 31 and 101 ($n = 16$), see text for explanations. The stars and corresponding values represent the best estimation for the intersection. The site number is indicated close to each small circle.

formed, but just initiating in the south, near the periclinal termination of the anticline (Fig. 11b). The westernmost sites (9 and 10) were almost horizontal. In the western limb of the anticline, we observe a progressive decrease of the Hercynian dip from north to south. To the north in the area of Aïn Chebbi (Figs 1b and 11b), the Hercynian dip was already exceeding 35° (about 50 per cent of the present dip), which is a little too high, compared to the present tilt of the Jurassic conglomerate. It was 28° in site 101, and southwards (sites 2 and 3) it was close to horizontal. The eastern limb of the anticline presented the same decrease of the Hercynian dip from north to south (about 40° in sites 22, 23 and 31, 22° in site 105 and 3° in site 103). The secondary fold close to site 103 possibly was not yet formed. Further south, in the periclinal termination, site 104 on the western limb and sites 4, 5 and 20 on the eastern limb belong to the same block delimited by two NE–SW trending faults (Figs 1b and 11a). Here, the incipient Hercynian anticline is clear, even if the absolute dips are small (Fig. 11b and Table 3).

*Effects of the second tectonic phase* ($\varphi 2$): The proportion of tilting related to $\varphi 2$ in this part of the Reggane Basin is not homogeneous from one group of sites to the other, but is overall more important than the Hercynian one (Fig. 11 b and Table 3), in agreement with the proportional unfolding of the 20 sites. However, at sites 101

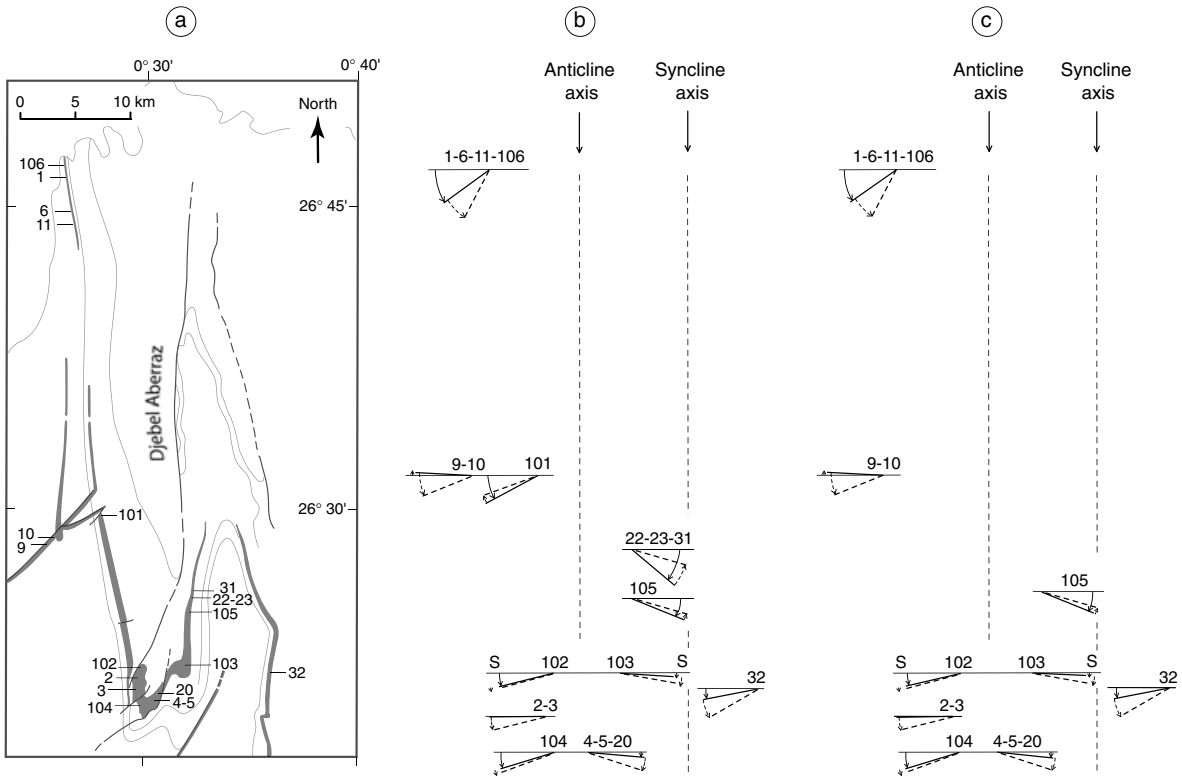


**Figure 11.** Cartoon representing the two tilting events having occurred, respectively, before (Hercynian dips, full black lines) and after (doted lines) the dolerite emplacement (see also Table 3). The relative longitudinal and latitudinal position of the sites represented in the sketch map of Fig. 1(b) is preserved in Figs (b) and (c). (a) Sketch map of the area. (b) Assumption 1 (all the sites). (c) Assumption 2 (l6 sites).

and 105-22-23-31, this second event would have reduced the tilt produced by the first phase.

To explain the dip reduction in sites 101 and 105, 22, 23, 31, we rather favour the role of local perturbations superimposed on the general structural trends of the studied area, probably in relation with the activity of secondary faults. For the group of sites (105-22-23-31), the dip reduction during $\varphi 2$ could stem from secondary refolding inside the pinched area situated east of the southern termination of the Djebel Aberraz anticline (Fig. 1b). Indeed, the main part of the Djebel Aberraz anticline is thrusted eastward over its eastern limb through a large N–S fault (see Figs 1b, c and (a). Around sites 22-23-31, and to a lesser degree site 105, a refolded syncline-anticline structure could have formed during the post-dolerite compressive event, as suggested by the two corresponding periclinal terminations observed further south, around site 103 (Figs 1b, 1c and 11a). As sites 105, 22, 23 and 31 belong to the eastern limb of the main anticline, the secondary syncline-anticline axes would run west from these sites, so that their dip could have been reduced as a result of the refolding process.

### Assumption 2 : sites 101, 22, 23 and 31 are discarded ($N = 16$ sites)

Assumption 1 takes into account several sites in which the Hercynian dip would have been higher than the dip observed today on the field (site 101 and sites 22, 23, 31 and 105). It means that the second tectonic event would have reduced the previous tilt of the strata. In a general context of transpression, a dip decrease of already inclined strata is not expected but can occur, if for instance the site is adjoining a fault and is locally disturbed by its activity.

Site 101 is situated in the sill next to a small transverse fault and to the intersection with the dike. With a Hercynian dip of 28° while the present dip is 20°, its tectonic behaviour is discordant with respect to all the other sites of this limb (Fig. 11b). Here, one must call upon a local fault effect, which would not reflect the regional tectonics.

A possible explanation has been proposed for sites (22, 23, 31 and 105) in terms of a slight refolding of the eastern limb of the main anticline. However, assumption 1 assumes that the magnetization direction of sites (22, 23, 31 and 105) has faithfully recorded the Early Jurassic field. We previously explained why we have doubts about the quality of the ChRMs of sites 22, 23 and 31, whereas the direction of the C Component seems to be more reliable at site 105. Indeed, sites 23 and 31 enlarge the area of the small circles intersection (Fig. 10a), increasing the uncertainty around the intersection direction. Such a large stripe of small circles has been observed in almost cylindrical folds (Cairanne *et al.* 2002; Henry *et al.* 2004a) but suggests that the ChRM of certain sites is questionable for one of the following reasons: error in the strike measurements, the two tectonic phases are not collinear or the ChRM itself is not reliable. Here, a biased ChRM direction is likely to explain why several arcs of circle, joining the directions before and after tectonic correction, evolve outside of the main intersection area (sites 101, 22, 23 and 31, Fig. 10a). Also, it is worth noting that the mean direction recorded in sites 22 and 31 is based on 3 samples only (Table 2), while the neighbour site 30 has been discarded because no reliable ChRM could be isolated.

Including these particular sites in the calculation strongly forces the intersection declination, respectively, to the east (sites 22-23-31) and to the west (site 101). For all these reasons, we will discard sites 22, 23, 31 as also 101 in the next calculation.

**Table 3.** Dips (in degrees) acquired in each site during first the Hercynian phase, Φ1, then the post-dolerite phase, Φ2, as calculated from the small circles best intersections, in the two cases considered in the text: Assumption 1, for all the 20 sites. Assumption 2, for 16 sites. Dips Φ1 correspond to the dips of the sites at the time of the dolerite intrusion. Negative dips for Φ1 and Φ2 mean that after the Hercynian phase the layer was tilted in the opposite direction than the present one, and that during the post-dolerite event the previous Hercynian dip has decreased (the final dip should always be the algebraic sum of the dips resulting from Φ1 + Φ2).

| Site | Present dip | | Assumption 1 | | Assumption 2 | |
|---|---|---|---|---|---|---|
| | Azimuth | Dip | Dip Φ1 | Dip Φ2 | Dip Φ1 | Dip Φ2 |
| 1 | 265 | 65 | 31 | 34 | 30 | 35 |
| 106 | 260 | 60 | 42 | 18 | 41 | 19 |
| 6 | 261 | 65 | 29 | 36 | 28 | 37 |
| 11 | 262 | 60 | 42 | 18 | 42 | 18 |
| 9 | 282 | 22 | −4 | 26 | −4 | 26 |
| 10 | 282 | 22 | −2 | 24 | −2 | 24 |
| 101 | 245 | 20 | 28 | −8 | — | — |
| 102 | 160 | 15 | 14 | 1 | 13 | 2 |
| 2 | 274 | 14 | −1 | 15 | −1 | 15 |
| 3 | 274 | 14 | 2 | 12 | 2 | 12 |
| 104 | 284 | 20 | 17 | 3 | 17 | 3 |
| 32 | 273 | 30 | 11 | 19 | 11 | 19 |
| 4 | 126 | 17 | 5 | 12 | 5 | 12 |
| 5 | 126 | 17 | 4 | 13 | 3 | 14 |
| 20 | 121 | 20 | 9 | 11 | 9 | 11 |
| 103 | 177 | 10 | 3 | 7 | 3 | 7 |
| 105 | 105 | 16 | 22 | −6 | 22 | −6 |
| 22 | 95 | 16 | 38 | −22 | — | — |
| 23 | 95 | 16 | 41 | −25 | — | — |
| 31 | 98 | 15 | 41 | −26 | — | — |

The small circles become more tightly grouped (Fig.10b) and the expected direction better defined than in the previous case. The intersection direction, $D = 326.7^\circ, I = 27.1^\circ, \alpha_{95} = 1.4^\circ, k = 671$, is not significantly different from the previous one nor from the direction obtained for 46 per cent of a proportional untilting ($D = 328.0^\circ, I = 28.7^\circ, \alpha_{95} = 1.4^\circ, k = 65.1$). The general geometry of the structure during the dolerite intrusion remains globally unchanged, but it is more regular after each one of the tectonic events than in the previous assumption (Fig. 11c), and the dips are slightly lower in the Aïn Chebbi area, in better agreement with the present dip of the conglomerate. The dip of site 105 during the intrusion is notably reduced, although still 6° higher than the present dip, consistent with a possible slight refolding of the structure.

The VGP corresponding to the intersection of the 16 sites taken into account is situated at $\lambda_p = 56.6^\circ$N, $\varphi_p = 255.8^\circ$E ($\lambda_p = 57.6^\circ$N, $\varphi_p = 254.3^\circ$E° for 20 sites). We now compare this VGP with the 200 Ma palaeopole drawn from the master curve of Besse & Courtillot (2003) for South Africa, after transfer into NW African coordinates. Our VGP is only 6.5° or 4.8° away, if we use the rotation parameters of, respectively, Fairhead (1988) and Nürnberg & Müller (1991). These differences are not significant and can be accounted for both by the relatively large area of the small circles intersections and by the secular variation, because these volcanic rocks represent a snapshot in the recording of the Early Jurassic Earth magnetic field.

Whatever the assumption (20 or 16 sites), the second tectonic event is compatible with the sinistral transpressive movement along the faults, as proposed by Conrad (1981), also inferred from the geological map (Bensalah *et al.* 1972) and evidenced by Guiraud & Maurin (1992) for the play of the West African N–S trending fault zones during Neocomian to Barremian times.

This study confirms that, in the Reggane basin, when the dolerite was intruded, the Palaeozoic sediments were neither horizontal nor folded as today, but partly tilted. The Hercynian tectonic phase produced only an incipient anticline-syncline structure with a slightly south dipping axis. Subsequently, the post-dolerite phase increased notably the folding, leading to the folds we can observe today (Fig. 1b). Likely, old Pan-African fractures were reactivated first as dextral transpressive faults during the Hercynian phase (Haddoum *et al.* 2001), then with a sinistral movement during the post-dolerite tectonic event (Guiraud & Maurin 1992), allowing for a differential tilting of neighbour parts of the fold, but with an overall coherent trend inside the same limb.

The age of the post-dolerite event is not well constrained, between the probably Late Jurassic continental Formation and the 'Continental Intercalaire' Formation of Early Cretaceous age in this area (De Lapparent 1960; Conrad (1981), Lefranc & Guiraud (1990)). It can be a far-field effect of the Cimmerian tectonic phase (around 145–140 Ma) which strongly affected the south-eastern part of the Eurasian plate at the beginning of the Early Cretaceous. It could also correspond to the Late Barremian to earliest Aptian rifting phase (Austrian phase, around 120–130 Ma) which reactivated the N–S trending faults of the Algeria-Libya-Niger confines as sinistral strike-slip faults, generating local drag folds and pull-apart basins (Guiraud & Maurin 1991, 1992; Boote *et al.* 1998). In a more general geodynamic context, this later tectonic phase corresponds to the onset of drifting of the South American plate away from the African–Arabian one. As a result of the overall tensional stress regime, the African–Arabian plate started to subdivide into three major blocks: Western block, Arabian-Nubian block and Austral block, with a sinistral strike-slip movement between the Western Block and the Arabian-Nubian Block (Fairhead 1988; Unternehr *et al.* 1988; Guiraud & Maurin 1991, 1992; Nürnberg & Müller 1991; Guiraud *et al.* 2005).

## CONCLUSION

The folded and faulted structures observed in the North Western Saharan platform are usually considered to be mainly a consequence of the Hercynian orogeny developed at the African–Laurussian plate margins in the Late Palaeozoic. While many local geological observations all over Africa and Arabia indicate that several tectonic events occurred in the Mesozoic Era, it was generally accepted that these effects were limited (block tilting, minor unconformities, drag folds along the reactivated faults). The present study, based on a palaeomagnetic analysis, provides tectonic information independent but complementary to the geological observations. The study was performed in the Reggane Basin because, in this particular area, a doleritic sill of Liassic age intrudes folded Palaeozoic sediments. This favourable situation allowed a fold test, based on the intersection of the small circle analysis, to be performed, leading to the reconstruction of the fold geometry at the time of the dolerite intrusion. The small circle analyses proved to be an efficient method to quantify the tectonic phases having occurred in the Reggane Basin before and after the dolerite intrusion. The results show that, the Hercynian phase initiated the folds, producing a limited tilt of the strata. The post-dolerite tectonic event was more important and increased significantly the structuration of the fold.

This work reveals the importance of a post-dolerite tectonic event, likely a far-field stress effect of either the Cimmerian (∼140 Ma) or

the Austrian (∼125 Ma) tectonic phase, together with the synsedimentary play during the whole Neocomian-Barremian rifting phase (Guiraud *et al.* 2005) in the Reggane Basin, as likely also in the surrounding basins. Although it cannot be precisely dated, this tectonic phase is probably a local consequence of the much larger scale major event of the break-up of Gondwana in the Late Barremian times, when South America started drifting away from Africa, while the rifts and fracture systems delimited three large blocks in the African plate. This study provides further evidence that tectonic stresses concentrated at the plate margins can be transmitted to distant intracontinental plate domains, as stated by Zoback & Zoback (1989).

## ACKNOWLEDGMENTS

This work was supported by the French-Algerian Cooperation agreement (CMEP Projec 95 MDU 332), CNRS—Université Montpellier 2 and CRAAG (Algiers). We are very grateful to the Algerian D.G.R.U. of the M.E.R.S. and to the French Foreign Office. We are indebted to A. Moussine Pouchkine for many constructive geological discussions on the Reggane and Ahnet Basins. We thank R. Guiraud, M. Brunel, J. F. Ritz and P. Labaume for valuable discussions about the geological implications of our study. We also thank the SONATRACH, IFP and REPSOL managements for allowing us to publish some of these data. This is also a contribution to IGCP485. Finally, this manuscript was notably improved thanks to the constructive criticism of R. Guiraud and D. van Hinsbergen.

## REFERENCES

Bailey, R.C. & Halls, R.C., 1984. Estimate of confidence in paleomagnetic directions derived from mixed remagnetization circle and direct observational data, *J. Geophys.,* **54,** 174–182.

Bardon, C., Bossert, A., Hamseh, R. & Westphal, M., 1973. Etude paléomagnétique de formation du Trias et du Jurassic du Maroc et du Sahara, *C. R. Acad. Sci., Paris,* **276,** 2357–2360.

Bazhenov, M.L. & Shipunov, S.V., 1991. Fold test in paleomagnetism: new approaches and reappraisal of data, *Earth planet. Sci. Lett.,* **104,** 16–24.

Bensalah, A. *et al.*, 1972. Carte Géologique de l'Algérie au 1/200 000: Feuille Reggane, BEICIP-SONATRACH-Service de la carte géologique de l'Algérie, Alger.

Bertrand, H. & Westphal, M., 1977. Comparaisons géologiques et paléomagnétiques des tholéiites du Maroc et de la côte orientale de l'Amérique du Nord : implications pour l'ouverture de l'Atlantique, *Bull. Soc. Géol. France,* **7**(XIX, 3), 513–520.

Besse, J. & Courtillot, V., 2003. Correction to "Apparent and true polar wander and the geometry of the geomagnetic field over the last 200 Mar" (vol 107, art no 2300, 2002)—art. no. 2469, *J. Geophys. Res. Solid Earth,* **108**(B10), 2469, doi:10.1029/2003JB002684.

Beuf, S., Biju-Duval, B., De Charpal, O., Rognon, P., Gariel, O. & Bennacef, A., 1971. Les grès du Paléozoïque inférieur au Sahara. Sédimentation et discontinuités. Evolution structurale d'un craton, in *Sci. techn. pétr.*, Publ. Inst. Fr. Petrol., Technip, Paris, **18,** 480.

Black, R. & Girod, M., 1970. Late Palaeozoic to Recent igneous activity in West Africa and its relationship to basement structure, in *African Magmatism and Tectonics*, Edinburgh, 185–210.

Black, R., Caby, R., Moussine-Pouchkine, A., Bayer, R., Bertrand, J.M.L., Boullier, A.M., Fabre, J. & Lesquer, A., 1979. Evidence for Late Precambrian plate tectonics in West Africa, *Nature,* **278,** 223–227.

Boote, D.R.D., Clark-Lowes, D.D. & Traut, M.W., 1998. Palaeozoic petroleum systems of North Africa, in *Palaeozoic petroleum systems of North Africa*, Geological Society, Special Publication, London, **132,** 7–68.

Buddington, A.F. & Lindsley, D.H., 1964. Iron-Titanium oxide minerals and synthetic equivalents, *J. Petrol.,* **5,** 310–357.

Caby, R., 1987. The Pan-African belt of West Africa from the Sahara desert to the gulf of Benin, in *The anatoMa of the Mountain Ranges*, Princeton Univ. Press, Princeton, 129–170.

Caby, R., Bertrand, J.M.L. & Black, R., 1981. Pan-African ocean closure and continental collision in the Hoggar-Iforas segment, central Sahara, in *Precambrian Plate Tectonics*, Vol. 16, pp. 407–434, ed. Kröner, A., Elsevier, Amsterdam.

Cairanne, G., Aubourg, C. & Pozzi, J.P., 2002. Syn-folding remagnetization and the significance of the small circle test. Examples from the Vocontian trough (SE France), *Phys. Chem. Earth,* **27,** 1151–1159.

Carslaw, H.S. & Jaeger, J.C., 1959. *Conduction of Heat in Solids*, 2nd edn, Clarendon Press, Oxford, p. 510.

Cebria, J.M., Lopez-Ruiz, J., Doblas, M., Martins, L.T. & Munha, J., 2003. Geochemistry of the Early Jurassic Messejana-Plasencia dyke (Portugal-Spain); implications on the Origin of the Central Atlantic Magmatic Province, *J. Petrol.,* **44,** 547–568.

Cogney, G., Termier, H. & Termier, G., 1971. Sur la présence de pillow-lavas dans le basalte du Permo-Trias au Maroc central, *C. R. Acad. Sci., Paris,* **273,** 446–449.

Conrad, J., 1972. Distension jurassique et tectonique éocrétacée sur le Nord-Ouest de la plate-forme africaine (Bassin de Reggan, Sahara central), *C. R. Acad. Sci., Paris,* **274**(14), 2423–2426.

Conrad, J., 1981. La part des déformations posthercyniennes et de la néotectonique dans la structuration du Sahara central algérien, un domaine relativement mobile de la plate-forme africaine, *C. R. Acad. Sci., Paris,* **292,** 1053–1056.

Conrad, G. & Lemosquet, Y., 1984. Du craton vers sa marge: évolution sédimentaire et structurale du bassin Ahnet-Timimoun-Béchar (Sahara algérien) au cours du Carbonifère; données paléoclimatiques, *Bull. Soc. Géol. France,* **26**(6), 987–994.

Conrad, J. & Westphal, M., 1973. Palaeomagnetic results from the Carboniferous and the Jurassic of the Saharan platform, in *Gondwana Geology*, Australian National University Press, Canberra, 9–13.

Dalrymple, G.B., Grommé, C.S. & White, R.W., 1975. Potassium-Argon age and paleomagnetism of diabase dikes in Liberia : initiation of central Atlantic rifting, *Geol. soc. Am. Bull.,* **86,** 399–411.

Delaunay, S., Smith, B. & Aubourg, C., 2002. Asymmetrical fold test in the case of overfolding : two examples from the Makran accretionary prism (Southern Iran), *Phys. Chem. Earth,* **27,** 1195–1203.

Donzeau, M., Fabre, J. & Moussine-Pouchkine, A., 1981. Comportement de la dalle saharienne et orogénèse varisque. Essai d'interprétation, *Bull. Soc. Hist. Nat. Afr. Nord,* **69**(3&4), 137–172.

Fabre, J., 1976. *Introduction à la géologie du Sahara algérien et des régions voisines*, Société Nationale d'Edition et de Diffusion, Alger, 422.

Fabre, J., 1988. Les séries paléozoïques d'Afrique: une approche, *J. African Earth Sci.,* **7,** 1–40.

Fairhead, J.D., 1988. Mesozoic plate tectonic reconstructions of the central South Atlantic Ocean: the role of the West and Central African rift system, *Tectonophysics,* **155,** 181–191.

Fisher, R.A., 1953. Dispersion on a sphere, *Proc. R. Soc. London,* **217,** 295–305.

Graham, J.W., 1949. The stability and significance of magnetism in sedimentary rocks, *J. geophys. Res.,* **54,** 131–168.

Guiraud, R. & Bellion, Y., 1995. Late Carboniferous to recent geodynamic evolution of the West Gondwanian, cratonic, Tethyan margins, in *The ocean basins and margins*, Plenum Press, New York, 101–124.

Guiraud, R. & Bosworth, W., 1999. Phanerozoic geodynamic evolution of northeastern Africa and the northwestern Arabian platform, *Tectonophysics,* **315,** 73–108.

Guiraud, R. & Maurin, J.C., 1991. Le rifting en Afrique au Crétacé inférieur : synthèse structurale, mise en évidence de deux étapes dans la genèse des bassins, relation avec les ouvertures océaniques péri-africaines, *Bull. Soc. Géol. France,* **162**(5), 811–823.

Guiraud, R. & Maurin, J.C., 1992. Early Cretaceous rifts of Western and Central Africa: an overview, *Tectonophysics,* **213,** 153–168.

Guiraud, R., Bellion, Y., Benkhelil, J. & Moreau, C., 1987. Post-hercynian tectonics in Northern and Western Africa, *Geol. J.,* **22**(Thematic issue), 433–466.

Guiraud, R., Bosworth, W., Thierry, J. & Delplanque, A., 2005. Phanerozoic geological evolution of Northern and Central Africa: An overview, *J. Afr. Earth Sci.,* **43,** 83–143.

Haddoum, H., Guiraud, R. & Moussine-Pouchkine, A., 2001. Hercynian compressional deformations of the Ahnet-Mouydir Basin, Algerian Saharan Platform: far-field stress effects of the Late Palaeozoic orogeny, *TerraNova,* **13**(3), 220–226.

Haggerty, S.E., 1976. Opaque mineral oxides in terrestrial igneous rocks, in *Oxide minerals, Short Course Notes*, Mineralogical Society of America, Washington DC.

Hailwood, E.A. & Mitchell, J.G., 1971. Palaeomagnetic and radiometric dating results from Jurassic intrusions in South Morocco, *Geophys. J. R. astr. Soc.,* **24,** 351–364.

Halls, H.C., 1976. A least-squares method to find a remanence direction from converging remagnetization circles, *Geophys. J. R. astr. Soc.,* **45,** 297–304.

Halls, H.C., 1978. The use of converging remagnetization circles in palaeomagnetism, *Phys. Earth planet. Inter.,* **16,** 1–11.

Henry, B., Rouvier, H., Le Goff, M., Leach, D., Macquar, J.C., Thibieroz, J. & Lewchuk, M.T., 2001. Palaeomagnetic dating of widespread remagnetization on the southeastern border of the French Massif Central and implications for fluid flow and Mississipi Valley-type mineralization, *Geophys. J. Int.,* **145,** 368–380.

Henry, B., Rouvier, H. & Le Goff, M., 2004a. Using syntectonic remagnetizations for fold geometry and vertical axis rotation: the example of the Cevennes border (France), *Geophys. J. Int.,* **157,** 1061–1070.

Henry, B., Merabet, N., Derder, M.E.M. & Bayou, B., 2004b. Chemical remagnetizations in the Illizi Basin (Saharan craton, Algeria), *Geophys. J. Int.,* **156,** 200–212.

Johnson, R.J.E. & Van der Voo, R., 1989. Dual-polarity Early Carboniferous remagnetization of the Fisset Brook Formation, *Geophys. J.,* **97,** 259–273.

Jordanova, N., Henry, B., Jordanova, D., Ivanov, Z., Dimov, D. & Bergerat, F., 2001. Paleomagnetism in northwestern Bulgaria: geological implications of widespread remagnetization, *Tectonophysics,* **343,** 79–92.

Khouas, A., 1998. Les structures hercyniennes de Bled El Mass et Azzel Matti et le contexte structural des dolérites du Bassin de Reggane et de Bled El Mass et leurs influences sur les hydrocarbures, Mémoire d'Ingénieur d'Etat en Géologie, IST/USTHB, Alger, 128.

Kirschvink, J.L., 1980. The least-squares line and plane and the analysis of palaeomagnetic data, *Geophys. J. R. astr. Soc.,* **62,** 699–718.

Lapparent de, A.F., 1960. Les Dinosauriens du "Continental intercalaire" du Sahara central, *Mém. Soc. géol. Fr.,* **39**(88A), 1–58.

Le Goff, M., 1985. Description d'un appareil à désaimanter par champs alternatifs; élimination de l'aimantation rémanente anhystérétique parasite, *Can. J. Earth Sci.,* **22,** 1740–1747.

Lefranc, J.P. & Guiraud, R., 1990. The Continental Intercalaire of northwestern Sahara and its equivalents in the neighbouring regions, *J. African Earth Sci.,* **10**(1/2), 27–77.

Lindsley, D.H., 1991. Oxide minerals : Petrologic and magnetic significance, in *Reviews in Mineralogy*, Vol. 25, p. 509, ed. Ribbe, P.H., Mineralogical Society of America, Virginia.

Logan, P. & Duddy, I., 1998. An investigation of the thermal history of the Ahnet and Reggane Basins, Central Algeria, and the consequences for hydrocarbon generation and accumulation, in *Petroleum Geology of North Africa*, Vol. 132, pp. 131–155, eds Macgregor, D.S., Moody, R.T.J. & Clark-Lowes, D.D. Geol. Soc., Spec. Publ., London.

Lowrie, W., 1990. Identification of ferromagnetic minerals in a rock by coercivity and unblocking temperature properties, *Geophys. Res. Lett.,* **17,** 159–162.

Manspeizer, W., 1988. Triassic-Jurassic rifting and opening of the Atlantic: An overview, in *Triassic-Jurassic Rifting. Continental Breakup and the Origin of the Atlantic Ocean and Passive Margins. Developments in Geotectonics*, Vol. 22, pp. 41–79, ed. Manspeizer, W., Elsevier, Amsterdam.

McClelland-Brown, E., 1983. Palaeomagnetic studies of fold development and propagation in the Pembrokeshire old red Sandstone, *Tectonophysics,* **98,** 131–149.

McFadden, P.L., 1990. A new fold test for palaeomagnetic studies, *Geophys. J. Int.,* **103,** 163–169.

McFadden, P.L. & Jones, D.L., 1981. The fold test in palaeomagnetism, *Geophys. J. R. astr. Soc.,* **67,** 53–58.

McFadden, P.L. & McElhinny, M.W., 1988. The combined analysis of remagnetization circles and direct observations in palaeomagnetism, *Earth planet. Sci. Lett.,* **87,** 161–172.

Nürnberg, D. & Müller, R.D., 1991. The tectonic evolution of the South Atlantic from Late Jurassic to present, *Tectonophysics,* **191,** 27–53.

Sebaï, A., Feraud, G., Bertrand, H. & Hanes, J., 1991. $^{40}Ar/^{39}Ar$ dating and geochemistry of tholeiitic magmatism related to the early opening of the central atlantic rift, *Earth planet. Sci. Lett.,* **104,** 455–472.

Shipunov, S.V., 1997. Synfolding magnetization: detection, testing and geological applications, *Geophys. J. Int.,* **130,** 405–410.

Smith, B., Bonneville, A. & Hamzaoui, R., 1991. Flow duration of a dike constrained by palaeomagnetic data, *Geophys. J. Int.,* **106,** 621–634.

Stamatakos, J. & Hirt, A.M., 1994. Paleomagnetic considerations of the development of the Pennsylvania salient in the central Appalachians, *Tectonophysics,* **231,** 237–255.

Surmont, J., Sandulescu, M. & Bordea, S., 1990. Mise en évidence d'une réaimantation fini crétacée des séries mésozoïques de l'unité de Bihor (Monts Apuseni, Roumanie) et de sa rotation horaire ultérieure, *C. R. Acad. Sci., Paris,* **310**(II), 213–219.

Sutter, J.F., 1988. Innovative approaches to the dating of igneous events in the early Mesozoic basins of the eastern United States, in *Studies of the Early Mesozoic basins of the eastern United States*, Vol. 1776, pp. 194–199, eds Froelich, A.J. & Robinson, G.R.J., US Geological Survey Bulletin.

Tauxe, L. & Watson, G.S., 1994. The fold test: an eigen analysis appraoch, *Earth planet. Sci. Lett.,* **122,** 331–341.

Turcotte, D.L. & Schubert, G., 1982. *Geodynamics. Applications of Continuum Physics to Geological Problems*, John Wiley, New York, p. 450.

Unternehr, P., Curie, D., Olivet, J.L., Goslin, J. & Beuzart, P., 1988. South Atlantic fits and intraplate boundaries in Africa and South America, *Tectonophysics,* **155,** 169–179.

Verati, C., Bertrand, H. & Féraud, G., 2005. The farthest record of the Central Atlantic Magmatic Province into West Africa craton: Precise $^{40}Ar/^{39}Ar$ dating and geochemistry of Taoudenni basin intrusives (northern Mali), *Earth planet. Sci. Lett.,* **235,** 391–407.

Vogt, P.R. & Einwich, A.M., 1979. Magnetic anomalies and sea-floor spreading in the western Atlantic, and a revised calibration of the Keathly (M) geomagnetic reversal chronology, in *Initial Reports of the Deep Sea Drilling Project*, Vol. 43, pp. 857–867, eds Tucholke, B.E. & Vogt P.R., US Government Printing Office, Washington DC.

Watson, G.S. & Enkin, R.J., 1993. The fold test in paleomagnetism as a parameter estimation problem, *Geophys. Res. Lett.,* **20,** 2135–2137.

Westphal, M., Montigny, R., Thuizat, R., Bardon, C., Bossert, A., Hamzeh, R. & Roley, J.P., 1979. Paléomagnétisme et datation du volcanisme permien, triassique et crétacé du Maroc, *Can. J. Earth Sci.,* **16**(11), 2150–2164.

White, R.S., Spence, G.D., Fowler, S.R., McKenzie, D.P., Westbrook, G.K. & Bowen, A.N., 1987. Magmatism at rifted continental margin, *Nature,* **330,** 439–444.

Wilson, R.L. & Everitt, C.W.F., 1963. Thermal demagnetization of some carboniferous lavas for palaeomagnetic purposes, *Geophys. J. R. astr. Soc.,* **8,** 149–164.

Wilson, M. & Guiraud, R., 1998. Late Permian to Recent magmatic activity on the African-Arabian margin of Tethys, in *Petroleum Geology of North Africa*, Vol. 132, pp. 231–263, Geological Society, Special Publication, London.

Zazoun, R.S., 2001. La tectogenèse hercynienne dans la partie occidentale de l'Ahnet et la région du Bled El-Mass, Sahara Algérien: un continuum de déformation (Variscan deformation in the western Ahnet Basin and Bled El-Mass area, Algerian Sahara: a continuous strain), *J. African Earth Sci.,* **32,** 869–887.

Zoback, M.L. & Zoback, M.D., 1989. Tectonic stress field of the conterminous Unitd States, in *Geophysical Framework of the Continental United States*, Vol. 172, pp. 523–539, eds Pakiser, L.C. & Mooney, W.D., Geol. Soc. Am. Memoir.

Zijderveld, J.D.A., 1967. A.C. demagnetization of rocks: analysis of results, in *Methods in paleomagnetism*, Elsevier, Amsterdam, 254–286.